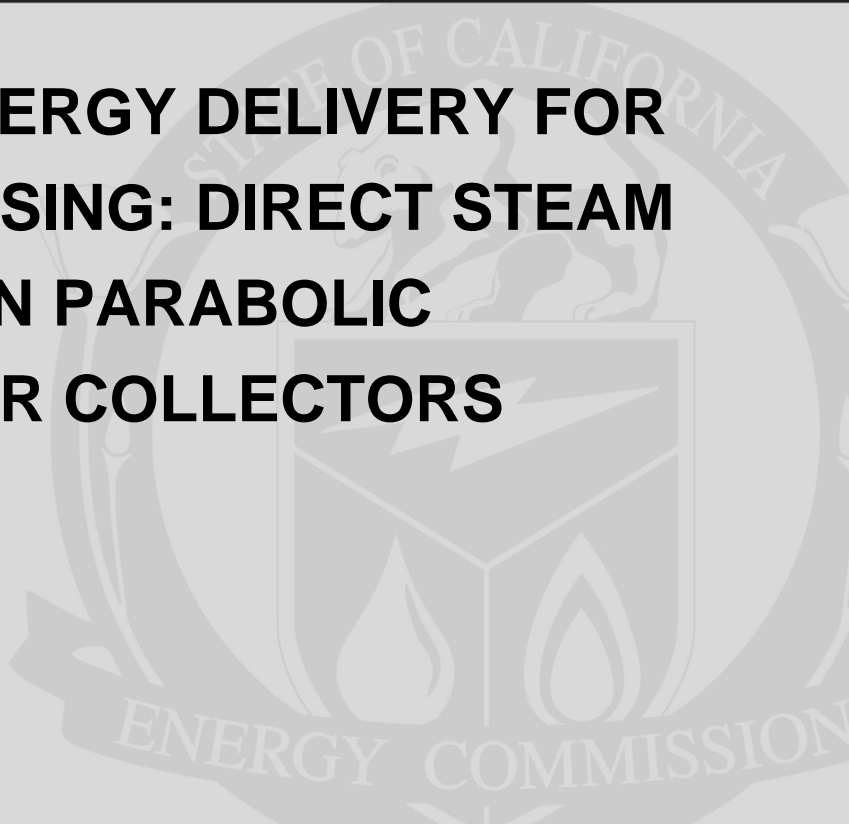


Energy Research and Development Division
FINAL PROJECT REPORT

**ADVANCED ENERGY DELIVERY FOR
FOOD PROCESSING: DIRECT STEAM
GENERATION IN PARABOLIC
TROUGH SOLAR COLLECTORS**



Prepared for: California Energy Commission

Prepared by: Abengoa Solar LLC

ABENGOA

AUGUST 2013
CEC-500-2014-073

Prepared by:

Primary Author(s):

E. Kenneth May
Angelo Chialva

Abengoa Solar LLC
11500 West 13th Avenue
Lakewood, CO 80215
303-928-8500
www.abengoasolar.com

Olivier Desjardins
Jeremy McCaslin

Sibley School of Mechanical and Aerospace Engineering
Cornell University, Ithaca, NY 14853

Contract Number: PIR-09-003

Prepared for:

California Energy Commission

Michael Lozano
Contract Manager

Virginia Lew
Office Manager
Energy Efficiency Research Office

Laurie Ten-Hope
Deputy Director
ENERGY RESEARCH AND DEVELOPMENT DIVISION

Robert P. Oglesby
Executive Director

DISCLAIMER

This report was prepared as the result of work sponsored by the California Energy Commission. It does not necessarily represent the views of the Energy Commission, its employees or the State of California. The Energy Commission, the State of California, its employees, contractors and subcontractors make no warrant, express or implied, and assume no legal liability for the information in this report; nor does any party represent that the uses of this information will not infringe upon privately owned rights. This report has not been approved or disapproved by the California Energy Commission nor has the California Energy Commission passed upon the accuracy or adequacy of the information in this report.

ACKNOWLEDGMENTS

The primary authors Ken May and Angelo Chialva acknowledge the support of the California Energy Commission in funding this work and Abengoa Solar Inc. for funding its participant cost share. We would also like to acknowledge the contribution of Professor Olivier Desjardins and his graduate student Jeremy McCaslin, from the University of Colorado, Boulder. Both are currently at Cornell University for their ground breaking contribution in applying Computational Fluid Dynamics to this complex problem of two-phase horizontal flow with thermal energy input.

PREFACE

The California Energy Commission Energy Research and Development Division supports public interest energy research and development that will help improve the quality of life in California by bringing environmentally safe, affordable, and reliable energy services and products to the marketplace.

The Energy Research and Development Division conducts public interest research, development, and demonstration (RD&D) projects to benefit California.

The Energy Research and Development Division strives to conduct the most promising public interest energy research by partnering with RD&D entities, including individuals, businesses, utilities, and public or private research institutions.

Energy Research and Development Division funding efforts are focused on the following RD&D program areas:

- Buildings End-Use Energy Efficiency
- Energy Innovations Small Grants
- Energy-Related Environmental Research
- Energy Systems Integration
- Environmentally Preferred Advanced Generation
- Industrial/Agricultural/Water End-Use Energy Efficiency
- Renewable Energy Technologies
- Transportation

This is the final report on the subject of Advanced Energy Delivery for Food Processing: Direct Steam Generation in Parabolic Trough Solar Collectors under grant award number PIR-09-003 conducted by Abengoa Solar LLC. The information from this project contributes to the Energy Research and Development Divisions's Industrial/Agricultural/Water End-Use Energy Efficiency

For more information about the Energy Research and Development Division, please visit the Energy Commission's website at www.energy.ca.gov/research/ or contact the Energy Commission at 916-327-1551.

ABSTRACT

Food processing is the third largest industrial energy user in California consuming 600 million therms of natural gas and 3,700 million kWh per year. This industry is a major user of low temperature heat and a prime target for using solar technology. Steam is a common mode of energy delivery in the industry and technologies to reduce solar steam costs will improve competitiveness in the market place.

Direct steam generation (DSG) in the absorber tube of a parabolic trough collector could reduce steam costs by increasing thermal output and reducing capital costs compared to existing technology. This report addresses the technical challenges of commercializing industrial DSG technology.

Abengoa Solar built a pilot plant for operational experience in DSG and to generate data to develop models that would be used in the design of commercial installations. Experiments under varying conditions of steam flow, pressure and solar radiation confirmed the performance advantages of DSG, demonstrated the stability of this process and discovered no mechanical issues that would preclude the industrial use of the technique.

Future work is required to develop theoretical correlations of the experimental data. These correlations would be used to design the pipe network of a commercial DSG plant and to test the stability of the network against flow excursions. The cost and performance of the commercial design would be compared against the parameters of conventional technology to determine the economic benefits of DSG technology.

A first commercial demonstration DSG plant would be necessary to accelerate the technology in the marketplace.

Keywords: California Energy Commission, solar collectors, solar concentrators, parabolic troughs, solar thermal, solar heat generation, solar steam generation, two phase flow, direct steam generation, computational fluid dynamics, food processing industry, renewable energy, industrial process heat, San Joaquin Valley

Report citation:

May, E. Kenneth; Chialva, Angelo. (Abengoa Solar LLC) 2013. *Advanced Energy Delivery for Food Processing: Direct Steam Generation in Parabolic Trough Solar Collectors*. California Energy Commission. Publication number: CEC-500-2014-073.

TABLE OF CONTENTS

ACKNOWLEDGMENTS.....	i
PREFACE	ii
ABSTRACT	iii
TABLE OF CONTENTS.....	iv
LIST OF FIGURES	v
LIST OF TABLES	vi
EXECUTIVE SUMMARY	1
Introduction	1
Project Purpose.....	1
Results.....	2
Benefits	3
CHAPTER 1 Introduction.....	5
1.1 Market Driven Potential of Solar Steam Generation.....	5
1.2 Lessons Learned from Industrial Solar Steam Generating Project	6
1.3 DSG Technology and Project Goals.....	7
CHAPTER 2 Direct Steam Generation Technology	10
2.1 Commercial Status	10
2.2 Technical Challenges to Commercialization.....	10
2.3 Technical Approach to the Challenges	13
2.3.1 Literature Survey.....	13
2.3.2 Theoretical Approaches	13
2.3.3 Pilot Plant Design.....	19
2.3.4 Pilot Plant Experimental Test Plan	20
2.3.5 Single Loop DSG Experiments.....	21
CHAPTER 3 Results	22
3.1 Computational Fluid Dynamics (CFD).....	22
3.1.1 Introduction	22

3.1.2	Colorado University Approach.....	23
3.1.3	Colorado University Results.....	23
3.2	Experimental DSG Program	26
3.2.1	Characterization of Test Loop with Liquid Flow	26
3.2.2	Impacts of DSG on Equipment.....	32
3.2.3	DSG Operations.....	35
3.3	Results of Single-Loop DSG Experiments	35
3.4	Results of Simulated Multi-Loop DSG Experiments	37
CHAPTER 4 Future Work.....		40
CHAPTER 5: Conclusions.....		41
GLOSSARY		42
APPENDIX A: References		A-1
APPENDIX B: First-Principle-Based Modeling of Direct Steam Generation Final Report....		B-1
APPENDIX C: Design of DSG Solar Pilot Plant.....		C-1
APPENDIX D: Results of DSG Experiments.....		D-1

LIST OF FIGURES

Figure ES-1 Direct Steam Generation Pilot Plant: Solar Collector Loop Generating Steam.....	2
Figure 1-1: Conventional Solar Steam Generation	7
Figure 1-2: DSG Solar Steam System.....	8
Figure 2-1: Flow Loop in a Potential Design of a Commercial DSG System	14
Figure 2-2: Flow Regime Map of Steam Generation at 10 Bar Pressure.....	15
Figure 2-3: Loop Mass Flow Rate (kg/sec) and Total System Pressure Drop (bar) for Different Steam Qualities.....	16
Figure 2-4: Thermodynamic Conditions vs. Flow Rate at 10 Barg Steam Delivery.....	18
Figure 2-5: Temperatures vs. Flow Rate at 10 Barg Steam Delivery	19
Figure 3-1: Two-Phase Flow Velocity Profiles in Pipe at High (85 bar) and Low (11 bar) Pressures.....	25
Figure 3-2: Two-Phase Flow in Pipe at High (85 bar) and Low (11 bar) Pressures Showing Film Thickness and Potential for Tube Dryout.....	26
Figure 3-3: Location of Pressure Transducers in DSG Flow Loop	27
Figure 3-4: Pressure in Flow Loop vs. Flow Rate	28
Figure 3-5: Measured vs. Predicted Pressure in Flow Loop	29

Figure 3-6: All Day Performance of the Collector Test Loop—Measured DNI (W/m²) and Thermal Efficiency (%) 30

Figure 3-7: Full Day Test Performance Test under Clear Sky Conditions—Solar Radiation, Measured and Predicted Thermal Energy Delivery 31

Figure 3-8: Full Day Test Performance Test under Clear Sky Conditions—Solar Loop Inlet and Outlet Temperatures..... 32

LIST OF TABLES

Table 2-1: Effect of Steam Pressure and Quality on Volumetric Flow..... 11

Table 2-2: Thermodynamic Conditions vs. Flow Rate at 10 Barg Steam Delivery 16

Table 3-1: Pump Discharge Pressure vs. Flow Rate 27

EXECUTIVE SUMMARY

Introduction

The food processing industry in California is a major consumer of energy. More than 600 million therms (60 trillion Btu) per year of natural gas are used to fuel thermal food processing operations that require relatively low temperature heat. This industry is an important target of the renewable energy industry to provide an economic alternative to fossil fuels that will also reduce green house gases and other pollutants. There are, however, numerous barriers to widespread installations of solar thermal technologies. These include lack of financial incentives that promote solar thermal technologies compared to other renewable energy technologies, the absence of credits to reduce air pollution and an industry unfamiliar with this technology, especially generating steam from solar.

Steam is a common form of delivering thermal energy to applications in the food processing industry. Typically low pressure steam, in the range of 50 – 150 pounds per square inch gage (psig) is needed, but sometimes medium pressure steam up to 300 psig is used. Using parabolic trough solar concentrators to generate steam at these temperatures is a good application.

In 2008, to introduce solar steam technology to the food processing industry and to demonstrate its potential to reduce fossil fuel use and air pollutants, the California Energy Commission provided funding to help install a ground breaking parabolic trough solar steam system at the Frito Lay plant in Modesto, California. This large system of more than 54,000 square feet of solar collectors is designed to produce all the required 300 psig steam used at the plant to heat the oil that is used to cook “Sun Chips”, a snack food. Although the Frito Lay solar system successfully generated the 300 psig steam, it was also expected to use existing conventional plant equipment to deliver that steam which increased its cost. This equipment included the unfired steam generator, the expansion tank and affected the cost of pumps, piping and fittings because of the increased temperature-pressure rating.

Project Purpose

For this project, researchers investigated the concept of using direct steam generation (DSG) for food processing. DSG was first promoted in the early 1980's in the United States as a way to reduce the cost of solar heat in industry. In the 1990's, the research and development focus shifted to Europe where DSG was promoted as a method to decrease the cost of electricity generated using parabolic trough collectors.

With DSG technology, steam is generated directly in the absorber tubes of a parabolic trough solar collector. The temperature and pressure of operations in the solar field would be close to the conditions required, and a steam separator tank would replace the unfired steam generator and expansion tank. DSG has the potential to reduce the cost of the equipment necessary for solar steam generation and increase thermal output. Both of these actions reduce the cost of solar generated steam and improve the competitive position of the technology compared to burning natural gas.

Results

This report addresses the technical challenges of commercializing DSG technology to produce industrial steam. The researchers surveyed the literature and found that correlations of two phase flow were the most relevant to use for this project. Even though these correlations were validated only for pressures greater than what is required for the parabolic trough solar collector, this research was the starting point for the analysis of low pressure DSG. To test these analyses, a pilot solar flow loop was built at Abengoa Solar's offices in Lakewood, Colorado to generate DSG data and gather operational experience (Figure ES-1).

Figure ES-1 Direct Steam Generation Pilot Plant: Solar Collector Loop Generating Steam



At the same time as this project, researchers at the University of Colorado, Boulder applied Computational Fluid Dynamic techniques to DSG. Computational Fluid Dynamics uses fundamental equations to analyze and solve problems in fluid mechanics. The University of Colorado work produced a computer visualization of two-phase fluid flow within a short section of the receiver tube and also predictions of tube dryout.

The experimental program initially characterized the system under liquid flow so that actual temperatures and pressures in the collector loop and solar measurements could be correlated with theoretical models. Numerous experiments were then conducted under different initial conditions of flow and steam pressure settings.

This experimental data confirmed that a DSG system:

- Operates at a lower pressure and lower temperature than a conventional solar steam-generating system.
- DSG has the potential to reduce system capital costs while at the same time delivering increased thermal energy output.
- The potential gains increase as the steam delivery pressure increases.
- The direct generation of steam is stable over a wide range of operating conditions and imposed perturbations brought about by changes in solar radiation and flow rate.
- There is no evidence of mechanical damage caused by DSG to solar system components.

The researchers concluded that further testing of these theoretical models is necessary and/or develop new ones to correlate actual data to theoretical models. These models would be used to design the pipe network of a commercial DSG plant and to test the response of the network to perturbations likely to be encountered in the field. The model will also be used as tool to test strategies to avoid tube dryout. The proposed commercial plant design would be used as the basis for economic and performance comparisons with conventional solar steam plants.

Benefits

Food processing is the third largest industrial energy user in the state and highly sensitive to energy price “shocks” which makes it a major target for energy strategies aimed at reducing green house gas and air pollution emissions. Renewable energy technologies have the potential to address both these issues.

As the DSG system is more accepted in the industry, coupling this technology with the parabolic trough solar collector can significantly reduce the capital costs of installed of solar systems, increase thermal performance and lower natural gas and electricity use.

CHAPTER 1

Introduction

1.1 Market Driven Potential of Solar Steam Generation

On Earth Day in April 2008, California Governor Arnold Schwarzenegger inaugurated a ground-breaking solar thermal system at the Frito Lay plant in Modesto, California. With a net collector area of 5,069 meters square (54,528 square feet), this was one of the largest process heat systems in the world and the first solar steam system to be installed in the US since the Department of Energy-funded demonstration projects in the early 1980's. The 300 psig, 422°F (20.7 bar, 217°C) steam solar generated heat is exchanged with the hot oil used to fry snack foods, such as "Sun Chips". The Modesto project was partially funded with an Energy Commission grant with the majority of financing from Frito Lay. The collector hardware was supplied by Abengoa Solar.

The Frito Lay project was driven by the desire to promote using alternative energy sources within the food processing industry. In addition, the San Joaquin Valley, where most of California's food growing and processing is concentrated, is a air pollution "non-attainment" area. Cleaner renewable energy instead of fossil fuels can contribute to improved air quality and protect human health.

The food processing industry in California is a major sector of the economy. In 2010, there were 3,412 establishments generating a food processing output (total costs for materials, labor, transportation, etc.) of \$66.5 billion.¹ Value added was \$26.7 billion for a total economic impact of \$93.2 billion. Direct employment totalled 157,585 people or about 866,000 people employed directly or indirectly servicing the California food processing industry.² The food manufacturing sector is expected to continue steady growth in employment by more than one percent per year.³

Food processing is the third largest industrial energy user in the state consuming 600 million therms of natural gas and 3,700 million kWh per year.⁴ This dependence on energy resources makes the industry highly sensitive to energy price "shocks" and a major target for energy strategies aimed at reducing green house gas and air pollution emissions. Renewable energy technologies have the potential to address both these issues.

¹ California Food Processing: A Powerhouse of Value: 2010, The McLean Group.

² The US Bureau of Economic Analysis uses a final-demand employment multiplier of 5.5 for Food Manufacturing products.

³ Northern California Center of Excellence and Office of Economic Development, Cerritos College, *Food Manufacturing in California 2010*.

⁴ California Energy Commission, Staff Report, *California's Food Processing Industry Energy Efficiency Initiative: Adoption of Industrial Best Practices*, January 2008.

Unlike many energy consuming sectors in California, such as oil extraction or petroleum refining, the food processing industry consumes heat at relatively low temperatures, typically between 140° – 450°F (60°– 230°C). Heat at these lower temperatures can be supplied by a number of solar thermal collector technologies, such as flat plates (heat delivery up to 160°F), evacuated tubes (up to 200°F) and parabolic trough solar concentrators (up to 500°F). Low pressure steam, between 50– 150 pounds per square inch gage (psig) and sometimes up to 300 psig is a common means of heat generation and distribution to drive food processing operations, such as cooking, frying, baking, drying, sterilization, pasteurization and washing. Generating steam for these conditions is suitable use of parabolic trough solar concentrators.

1.2 Lessons Learned from Industrial Solar Steam Generating Project

Operating the solar system at the Frito Lay, Modesto plant has been routine during the last five years. Much has been learned from the plant construction and operation, and from follow-up work promoting renewable energy systems in California’s food processing industry, mainly in the San Joaquin Valley. Such lessons include:

- Using steam as a heat transfer medium in the food processing industry is important.
- Understanding the disadvantages of the conventional approach to solar steam generation with system operating temperatures and pressures, and cost. The elevated temperatures and pressures of conventional solar steam generation reduce the efficiency of solar thermal systems and require using costly plant equipment. Equipment that reduces the thermal output and increases the cost of a solar system degrades the solar system competitiveness with conventional steam generation using fossil-fuel (usually natural gas) fired boilers
- Identifying the institutional barriers to commercialize solar heat technologies. Electric-generating technologies, such as PV (photovoltaics) in California are promoted by generating a certain amount of electricity from renewable sources usually coupled with considerable financial incentives. There are no directives to generate a certain amount of process heat from renewable sources and incentives to reduce the cost of solar thermal systems are limited.
- Solar thermal technologies receive no credit for reducing air pollution. A food processor cannot install a solar system to reduce NOX emissions as an alternative to installing low-NOX boilers that would provide the same amount of emission reduction.
- There are no federal programs promote solar thermal technologies in industry or provide funds for solar thermal R&D. (Food industry consumes about one-third of the natural gas consumed in the US. Natural gas makes up about one-quarter of the total energy consumed in the US and about one-third of US fossil fuel consumption.⁵ Funding by the Energy Commission of this project was a California state initiative aimed at reducing the cost of solar thermal technology to increase its competitive position in the energy field, and, specifically, in the food processing industry.

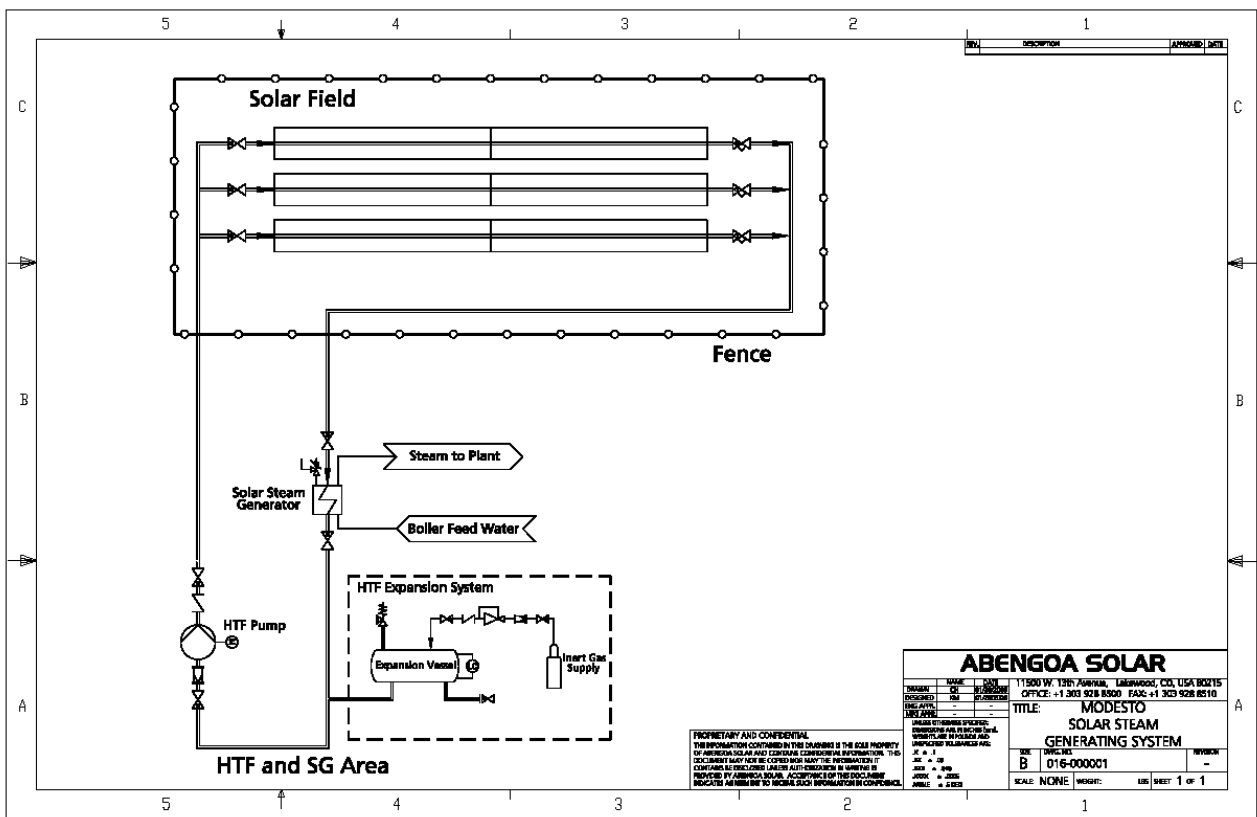
⁵ US Energy Information Administration, Annual Energy Review, September 2012.

1.3 DSG Technology and Project Goals

This R&D project addressed the technological and economic barriers that hinder using solar thermal technologies in California’s food processing industry. The researchers investigated commercializing Direct Steam Generation (DSG) technology to deliver saturated steam to industrial processes.

The conventional means of generating steam from solar technology uses a heat transfer fluid (oil or high-temperature, pressurized water) circulated through the solar field into an unfired steam generator (Figure 1-1). Inside this heat exchanger, boiler feed water changes phase and steam is delivered to the process plant.

Figure 1-1: Conventional Solar Steam Generation

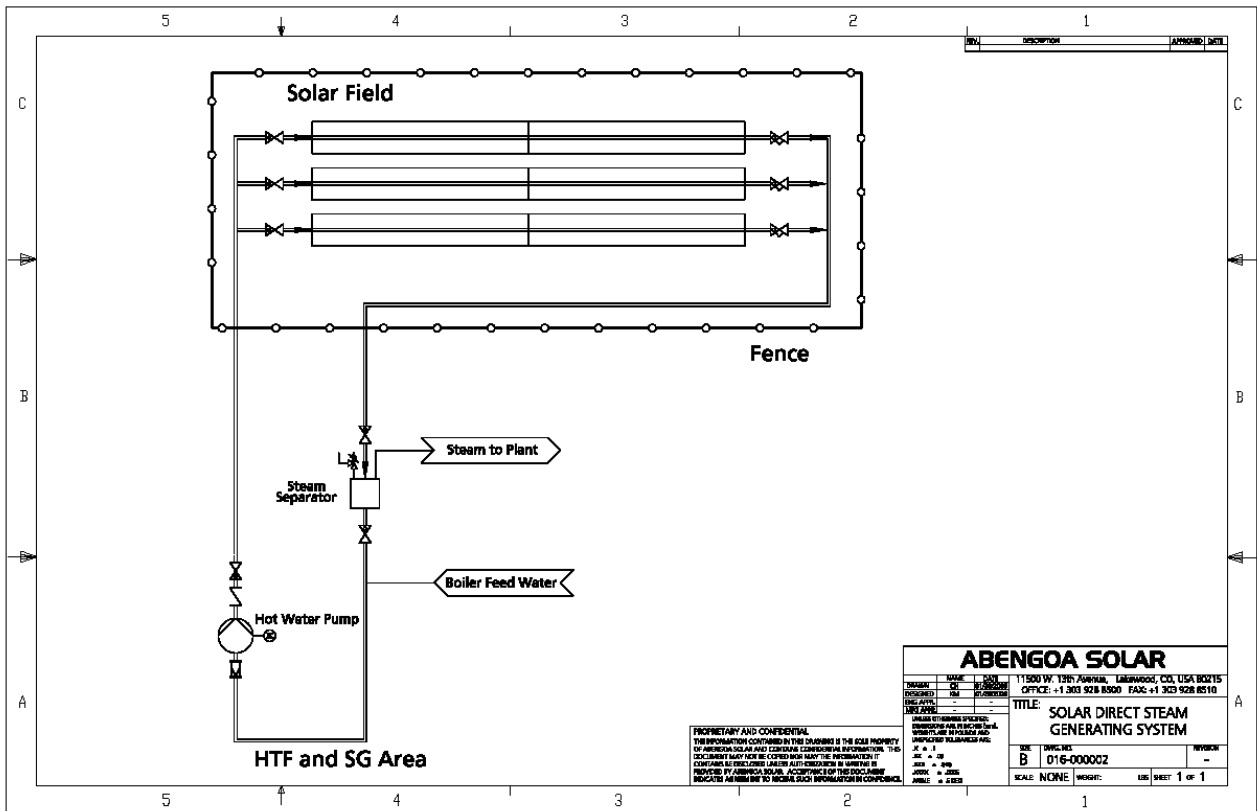


Since the solar field operates as a closed loop, an expansion tank is required to absorb thermal expansion while providing sufficient pressure to prevent boiling in the solar field. Because a differential temperature is required to drive the heat exchange process, the inlet temperature to the solar field is higher than the steam delivery temperature. The outlet temperature in the solar field is at a considerably higher temperature because of the solar energy input. Pressure in the solar field must be regulated to ensure there is no boiling in the collectors. This requires that the solar field pressure be much higher than the pressure of the steam generated. For the Frito Lay

system, the solar field design pressure at 600 psig (41.4 bar) is double the steam delivery pressure of 300 psig (20.7 bar). These elevated temperatures and pressures significantly impact the cost to balance the other plant equipment, such as the unfired steam generator, the expansion tank, the circulating pump and fittings, such as valves and pump strainers that require a high temperature/pressure rating. It also means for systems operating above 300 psig that flanged and welded connections will be used rather than less expensive threaded fittings that are made for less than 300 psig operations.

In a solar DSG system, water is allowed to boil in the receiver tubes (Figure 1-2). The two-phase mixture of steam and water is transported from the solar field to a steam separator. The steam flows into the steam header and the water is recirculated back through the solar field.

Figure 1-2: DSG Solar Steam System



Makeup boiler feed water from the process plant is injected into the steam separator to maintain a constant level.

For a DSG system, the expensive unfired steam generator is eliminated. The steam separator provides expansion capability to the open loop DSG system, but operates at the steam pressure, not at the higher pressure required to suppress boiling in the solar field. Pressures and temperatures in the solar field are closer to the steam conditions than the conventional approach. Pumps and fittings, therefore, come with a lower temperature-pressure rating, and

using threaded fittings is possible. Because the solar field operates at a lower temperature, system performance is greater compared to using the conventional approach.

Overall, it is estimated with increased performance and reduced equipment needs, the cost of steam produced by the solar field using DSG would be 25 percent less than using conventional technology, Murphy and May [55]. Continuing toward installing DGS systems would advance using solar thermal steam technology to displace the large amount of the fossil fuels consumed in the food processing industry and decrease air emissions.

CHAPTER 2

Direct Steam Generation Technology

2.1 Commercial Status

This project uses Direct Steam Generation technology to deliver saturated steam to industrial processes as a means of increasing performance and reducing the cost of solar-generated steam. DSG was first proposed in the early 1980's in the US as an industrial technology [55, 56]. However, changed political priorities at the time reduced US funding for renewables R&D and the technology did not progress.

In 1995, DSG became the focus of a major research effort in Europe aimed not for industrial applications, but at the utility electric market. Here the goal was to deliver high pressure steam (in excess of 100 bar), superheated to temperatures in excess of 400°C from parabolic trough solar collectors directly to a steam turbine for electricity generation. The attraction of this approach is that many of the limitations of the conventional organic heat transfer oils are eliminated and higher steam turbine efficiencies are possible since the steam is delivered at a higher temperature than through the use of an oil.

R&D into DSG technology for parabolic trough electric applications continues today involving companies based in Spain and in Germany. The first commercial solar electric DSG plant came on line in January 2012 located in Thailand. Steam is generated at 340°C to drive a 5 MW turbine delivering electricity to the grid. The prospect is that more and larger such plants will come on line. However, it has taken almost 20 years of research effort to bring such a small plant on line indicates the complexity of the problem.

2.2 Technical Challenges to Commercialization

Parabolic trough solar fields comprise a network of multiple parallel flow paths that are used to convey solar energy from the collector to the point of energy delivery. A broad goal in designing the piping network is to equalize mass flows through each loop. In a solar field employing a liquid medium, it is relatively easy to achieve uniform flow throughout the solar field, because the characteristics of single-phase, liquid flow are well known and pressure drop can be accurately calculated. Typically, collector flow loops are very long and the pressure drop through a loop is large compared to the pressure drop in the supply and return headers. In addition, for loops near the fluid source, valves can be used to introduce additional pressure drop to reduce flow in loops near the supply and hence force more flow into loops further from the point of supply. Fluid mechanics assists the balancing process since pressure drop increases with about the square of the flow rate.

However, for two phase flow, the effects of phase change on flow distribution are more complicated as it is dependent on many factors, and the maintenance of equal flows in two-phase flow piping networks is the major challenge in commercializing the technology. The challenge would appear to be more severe at the low steam pressures under investigation for

industrial applications compared to DSG for utility conditions. This is because at low pressures the density difference between water and steam is much greater than at high pressures and it is the fraction of vapor in the two-phase flow stream that drives pressure drop.

For instance the ratio of liquid to steam densities at 50 psig is 372:1 and at 150 psig is 144:1. This means that even at low steam qualities (mass of steam/mass of steam plus mass of water) there is a large increase in volume compared to flowing in the liquid phase at the same rate. This is illustrated in Table 2-1 for two different steam pressures and different steam qualities. It can be seen that the increase in volume is almost proportional to quality for a given steam pressure. Volumetric flow and mixture velocity increases greatly as steam pressure is reduced. The mixture specific volume ratio to that of water is the same as the ratio of all liquid to mixture velocity, assuming that the liquid and gas travel at the same velocity. In practical terms, if the liquid flow through the loop were around 16 gpm, the all liquid velocity would be about 2.5 ft/s. The mixture velocity at 5 Percent quality would increase 19.5 times to about 50 ft/s. The amount of liquid in the mixture declines to a small fraction at low pressure and even modest qualities.

Table 2-1: Effect of Steam Pressure and Quality on Volumetric Flow

Steam pressure, psig	Steam quality	liquid sp volume, ft3/lb	Gas sp volume, ft3/lb	Liquid density, lb/ft3	Gas density, lb/ft3	Volume of 1 lb of mix, ft3	Mixture sp vol compared to liquid	Volumetric fraction of liquid in mixture
50	0.01	0.01735	6.449	57.64	0.155	0.082	4.7	0.210
50	0.05	0.01735	6.449	57.64	0.155	0.339	19.5	0.049
50	0.1	0.01735	6.449	57.64	0.155	0.661	38.1	0.024
150	0.01	0.01823	2.625	54.85	0.381	0.044	2.4	0.407
150	0.05	0.01823	2.625	54.85	0.381	0.149	8.1	0.117
150	0.1	0.01823	2.625	54.85	0.381	0.279	15.3	0.059

The large increase in flow velocity is responsible for the large increase in pressure drop in two-phase flow compared to liquid flow. For liquid phase flow, pressure drop is proportional roughly to the square of velocity. For two phase flow the situation is more complicated. First, the vapor is compressible causing differences in behavior compared to a liquid, second is the impact of “flashing” as hot, two-phase mixture decreases in pressure. Flashing increases the amount of vapor without energy input. Finally, as steam is formed in the absorber the flow goes through a number of different flow regimes, all with their associated, but different pressure drop characteristics. Pressure drop increases for a given mass flow as the steam pressure is decreased. This suggests that the flow instabilities in a multi-loop solar field will be harder to manage the lower the operating steam pressure.

As the above discussion would suggest, and as will be confirmed in data presented later in this report, within a loop in a large solar field generating steam, the greater amount of steam

generated in the loop the more the pressure drop through the loop increases. Total mass flow through that loop, if not regulated in some manner, will decrease.

In a large solar field with many flow loops, there is constant interaction between the different loops that affects flow distribution through the loops and the centrifugal pump, with its own pressure drop/flow characteristics that is driving the flow. Consider the impact of a cloud on some of the loops in the solar field. Those loops shaded from the sun would run colder. For a liquid phase system, the only impact would be on system properties. This might slightly increase the pressure drop on the colder shaded loops and cause a slight reduction in flow through those loops. More flow would go through other loops in the system, but any increase is restrained by the fact that pressure drop in these loops increases with the square of the increase in mass flow.

For a steam-generating system, steam production in shaded loops would decrease. This would decrease the pressure drop through these loops and increase mass flow. Less flow would go through the un-shaded loops so steam quality in these loops would increase. Increased steam quality increases pressure drop in these loops, further reducing mass flow in the illuminated loops and pushing more flow through the shaded loops. This sequence feeds upon itself. From an operational point of view, the concern is that flow is reduced in some collector loops to such an extent, that there is very little water and so much steam in the absorber tubes that tube “dryout” results. It is even more complicated since dryout of a tube is not just a function of mass flow, but is also a function of the two-phase flow regime present inside the tube. Ideally, the annular flow regime should exist whereby the flow of vapor forces a film of liquid around the entire circumference of the tube. The least favorable regime is stratified flow whereby all the liquid is at the bottom of the tube with most of the tube wall devoid of liquid. Solar radiation on a dried out tube wall will limit heat transfer and could cause a significant increase in localized tube wall temperatures.

For solar electric applications that are operating at very high temperatures and pressures, tube wall dry out could cause immediate localized overheating. We have noted at high pressures that vapor generation has less impact on pressure drop than at lower pressures, but nevertheless active measures are taken in such plants to control flow distribution within the solar field. Typically, this is in the form of flow control valves at the entrance to each flow loop. Such valves and flow meters are expensive, but are amortized over a large collector area, since utility scale troughs are on a much larger scale than troughs designed for smaller industrial applications.

For industrial DSG applications, such active flow balancing techniques are probably not affordable. Hence, the challenge of this project is to devise system designs and operating strategies so that solar DSG plants run in a stable manner, while achieving the cost reductions needed to make the technology more competitive in the marketplace.

2.3 Technical Approach to the Challenges

2.3.1 Literature Survey

A comprehensive list of references on DSG related to the problem under investigation was compiled as part of this project and is presented in Appendix A. Much of the literature is derived from the nuclear industry and the use of boiling water reactors. The use of line-focus solar concentrators adds additional complications because of the impact of gravity on horizontal receivers, because solar heating is not uniform around the tubes and because the intensity of solar heating is far from uniform due to variations in the level of solar radiation and the impact of solar angles that are continually changing throughout the day. Furthermore, a solar plant has to startup and shutdown every day compared to conventional electric power plants that can run for years between shutdowns.

The report by Desjardins [Appendix B] includes a summary of the literature relating to CFD.

The simplest correlation of two-phase flow pressure drop uses the homogeneous model. This assumes that the liquid and gas phases move at the same velocity through the pipe and that the two phases are fully mixed. Therefore, the mixture is treated as if there is only one phase. The properties of the mixture are calculated based on the average properties of the individual phases. This model has been shown to work best near the critical point where the densities of the two phases are similar or when the mass velocity of the two-phase flow is very high so that the flow regime is either bubbly or misty flow – again essentially a homogeneous mixture.

The work most relevant to this R&D project is the paper published by Eck in 2005 [1]. This is strictly an empirical approach used to correlate experimental data. It is based on the correlations of Friedel and involves the use of a factor, derived by Friedel, applied to the single phase pressure drop so as to calculate pressure drop in two-phase flow.

The literature shows good agreement between Eck's model and the simplified homogeneous model at high pressures of around 100 bar. However, divergence between the two models increases at lower pressures with Eck's model predicting higher pressure drop than the homogenous model. The comparison to actual data is limited to a minimum of 30 bar due to the lack of published data at lower pressures.

2.3.2 Theoretical Approaches

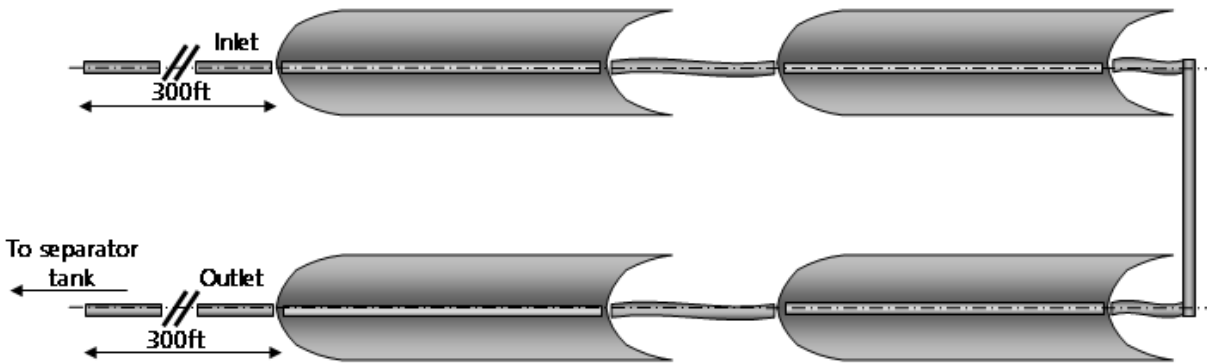
Eck's paper is the basis against which the experimental data generated during this project was compared. However, it was understood that the Eck correlations had never been compared against experimental data derived at less than 30 bar and that the range of steam pressures of interest for this research was in the range of 3 – 20 bar pressure.

ASI's modeling of DSG began with the coding of the Eck equations. This code was applied to the potential design of a commercial DSG installation. A single flow loop in a commercial system is shown in Figure 2-1. The loop is made up of 4, PT-1 collectors. Each collector consists of eight PT-1 modules and is 50 meters long.

The analysis provided important insights into the practical limits of DSG technology in terms of exit low-pressure steam qualities. In contrast to the generation of 100 bar steam where the goal

is exit qualities of 80 – 90 percent, the practical limit for the exit quality of low pressure steam appears to be in the range of 5 -10 percent. This limit arises because the pressure drop through the proposed collector loop is very great at low steam pressures. The modeling was also applied to the design of the pilot plant to specify the flow rate and head of the circulating pump, and the size of the loop return line. Finally, the analysis was used to give the Colorado University researchers a range of operational parameters over which to conduct their CFD research.

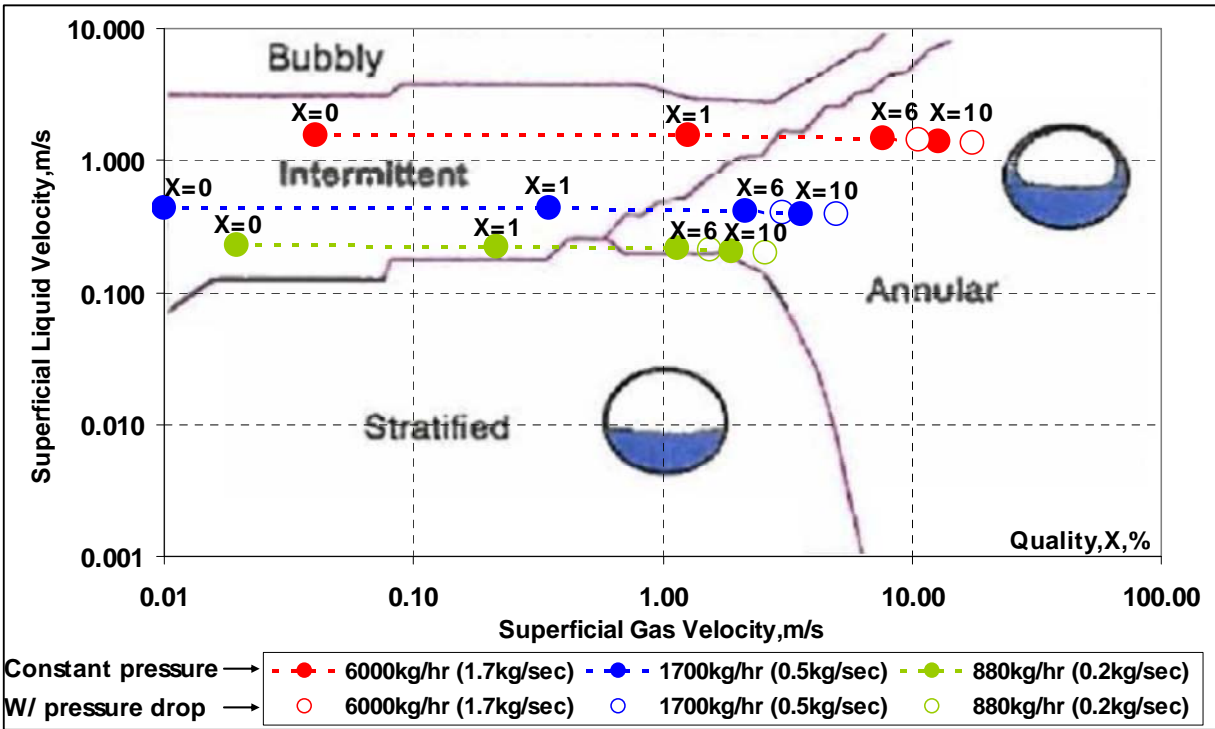
Figure 2-1: Flow Loop in a Potential Design of a Commercial DSG System



The preliminary modeling effort applying Eck’s equations to low pressure steam generation was used to plot the flow regime transitions through the flow loop. Superimposed on the flow regime map of Taitel and Dukler [24] in Figure 2-2 are the conditions in the solar loop from the beginning to the end of steam generation. Conditions are shown for a single pressure of 10 bar but at three mass flow rates, basically from the lowest to the highest practical flow rate through the loop.

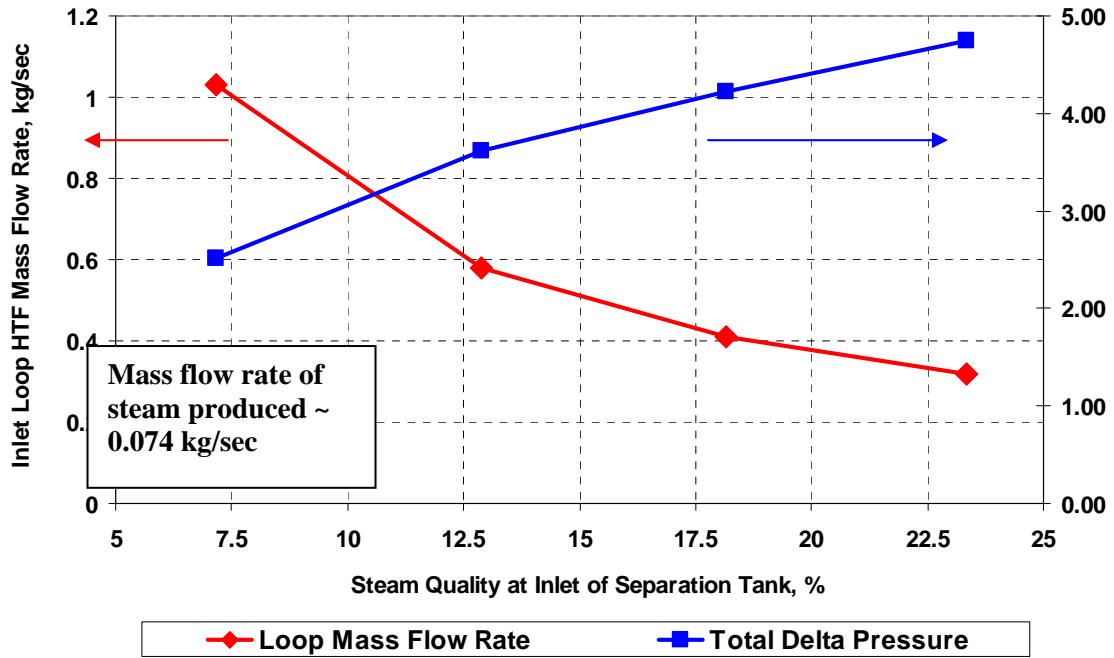
Except at the lowest flow rate, the progression of flow regimes (shown by the dotted lines) appears to be from the intermittent flow regime into annular flow. This avoids the stratified flow regime where dryout is most likely. The transition into the annular flow regime is desirable since it means that the tube wall is fully wetted and the potential for tube dryout reduced. However, this analysis was done only at 10 bar. At lower pressures with lower vapor densities, the results could be different.

Figure 2-2: Flow Regime Map of Steam Generation at 10 Bar Pressure



The theoretical approach was also applied to the pilot plant design where the number of collectors in the loop was half that proposed for a commercial installation. The results are shown in Figures 2-3 and Figures 2-4 and 2-5, again for the generation of 10 bar steam.

Figure 2-3: Loop Mass Flow Rate (kg/sec) and Total System Pressure Drop (bar) for Different Steam Qualities



The data were calculated up to a steam quality of 23 percent. This is probably beyond practical qualities for a commercial system, especially since the goal would be to use loops; at least twice as long as that employed in the pilot plant.

The results of further analysis of the pilot plant loop are shown in Table 2-1, and Figures 2-4 and 2-5 for exit steam qualities of 10 percent, 5 percent, and 1.8 percent at 10 bar gauge pressure (180C saturation temperature). Included in the pressure drop is 10 m each of supply and return piping at each end of the 100 meters of absorber tube. The contributions of the cross over piping and flexible hoses are not modeled.

Table 2-2: Thermodynamic Conditions vs. Flow Rate at 10 Barg Steam Delivery

Target quality	10% Steam Quality	5% Steam Quality	1.8% Steam Quality
Loop Water Inlet Temperature, C	180	180	180
Inlet Pressure, barg	14.23	13.38	12.25
Mass Flow Rate, kg/sec	0.54	0.92	1.73
Total Loop + Piping Pressure Drop, bar	4.23	3.38	2.25
Steam Quality at Separator Tank, %	13.32	7.82	4.18
Average Loop Temperature, C	192	189	185

Target quality	10% Steam Quality	5% Steam Quality	1.8% Steam Quality
Peak Loop Temperature, C	196	193	188
Loop Differential Temperature, C	16	13	8

The following observations are derived from the analysis.

- Exit steam quality is proportional to the inlet flow rate. Higher exit quality increases the overall pressure drop. Hence, higher quality increases pump head and loop inlet pressure, but reduces pump flow.
- The higher the steam quality and the lower the flow rate, the earlier steam generation begins in the loop. Conversely, at high flow rates, the capacity of the liquid phase to absorb energy is large so boiling occurs further along the loop.
- Pressure drop is low in the single phase flow regime. Single phase pressure drop is more significant for lower quality steam production (higher flow rates).
- The product: flow x differential pressure is an indication of pumping power. It decreases with increased quality. The largest decrease results from the first incremental decrease in flow rate. Hence, there is an incentive to reduce flow rates to reduce power consumption, the diameter on inlet lines to the solar field and potentially to reduce the cost of the pump. At the same time reduced flow will increase pressure drop and potentially require larger return lines from the solar field to the steam separator.
- Flashing due to the decline in absolute pressure along the tube contributes to steam generation and thus leads to increased pressure drop.
- The highest temperature in the loop occurs at the onset of boiling.
- Higher quality increases the maximum system temperature, although the difference between the extremes is not large: 196 to 188 C.
- In all cases, the average fluid temperature varies little from the steam delivery temperature; for these three cases a variation of 5 – 12 C above the delivered steam temperature.

Figure 2-4: Thermodynamic Conditions vs. Flow Rate at 10 Barg Steam Delivery

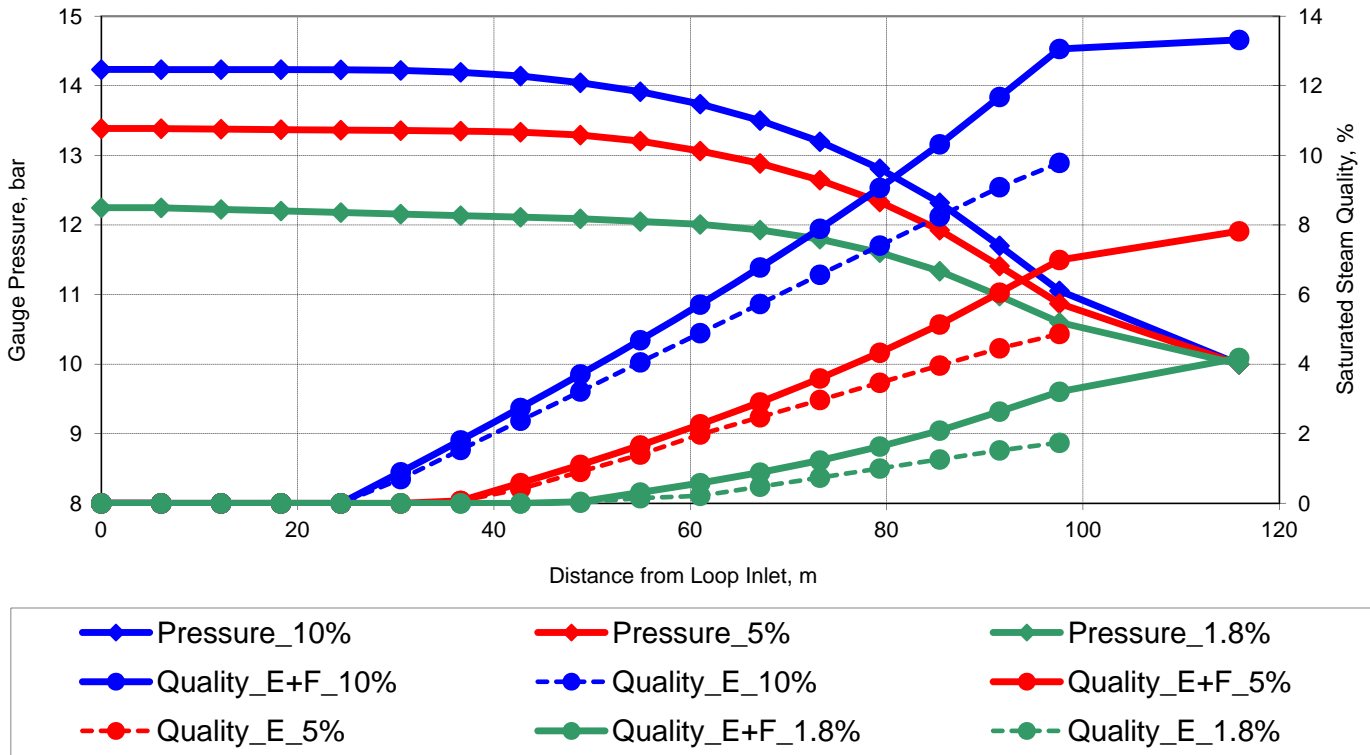
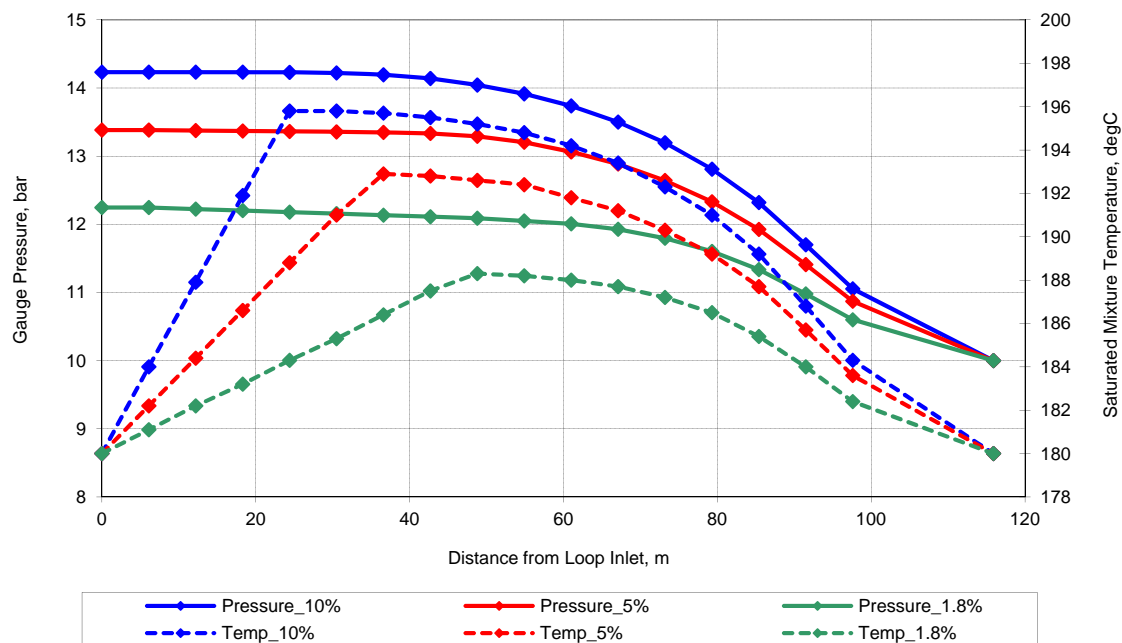


Figure 2-5: Temperatures vs. Flow Rate at 10 Barg Steam Delivery



2.3.3 Pilot Plant Design

There is essentially no published data on DSG at pressures less than 30 bar. This pressure is much higher than the pressure range of interest from about 50 to 300 psig (3.4 to 20.7 bar). Thus, as part of their cost share, Abengoa Solar designed and built a DSG pilot plant at their facility in Lakewood, CO. The goal of building and operating this pilot plant was to obtain data on steam generation at the low pressures of interest. This data would then be compared against existing models to test their validity. Should the models fail to conform to the experimental data, the goal would be to modify these existing correlations or to develop new correlations that are more accurate. An accurate means of calculating two-phase flow pressure drop is an essential element in being able to design commercial DSG plants.

The pilot plant design is shown in Appendix C. The system consists of two ASI, PT-1 parabolic trough collectors. Each collector consists of 8, PT-1 modules for a total net aperture area of 211 m². The collectors are arranged one in front of the other in two parallel rows. Piping is arranged so that the two collectors form a single flow loop with flow at one end down one collector, crossing over to the next collector and returning to supply end.

The system is highly instrumented with pressure transducers and temperature probes at the inlet, center and outlet of each collector. Additional pressure, temperature and flow measurements are taken around the circulating pump and steam separator tank. The tank is large enough to hold sufficient water for a full day of steam generation while still providing

sufficient disengaging space to delivery dry steam out of the top of the tank. The system can be run in a mode to generate and discharge steam to the atmosphere or in a single-phase mode where the solar heat is rejected through a fan coil heat exchanger to the air. A third mode allows a measured flow of water to be bypassed from the outlet of the pump back to the tank while the rest of the pump discharge flow passes through the solar loop.

A Campbell Scientific CR1000 data acquisition system was used to control the solar steam generating process, while collecting and processing the collected data. Such data was collected at intervals of each scan (about 6 seconds), and averaged over periods of one minute and one hour. In addition, critical variables were viewed and graphed in real time to ensure that everything was normal and that all instrumentation was recording correctly.

The solar field is arranged in an east-west orientation and hence can achieve normal incidence every day. Under peak conditions, the solar field will deliver about 430,000 Btu/h (127 kW) of thermal energy equivalent to about 500 lb/h (225 kg/h) of steam production. It was built with the capability of generating steam up to a pressure of 125 psig (8.8 bar). The goal was to conduct the experiments mainly at the peak part of the day within an hour or two of normal incidence under clear day conditions.

2.3.4 Pilot Plant Experimental Test Plan

An experimental test plan was created to guide the experimental program. It consisted of three parts:

- System characterization
- Single loop DSG steam production
- Simulated multi-loop steam production.

2.3.4.1 System Characterization

Characterization of the solar system was accomplished by operating the solar field as a pressurized water system in a close loop recirculation mode under various conditions of flow and temperature. The fan coil unit was operated to reject the heat generated while maintaining conditions in the solar loop as uniform as possible. The steam separator with a nitrogen blanket acted simply as an expansion tank.

Using liquid water that has very well defined thermodynamic properties, pressure drop as a function of flow rate was measured as well as system thermal performance and efficiency. Thermal energy delivery was calculated by measuring flow rate and differential temperature across the solar loop. Efficiency of the system was calculated using measurements of solar direct normal radiation recorded by the Abengoa Solar rotating shadow band pyranometer located at the site.

During DSG experiments, because of the phase change involved, it is not possible to measure thermal input by measuring differential pressure across the solar loop. However, for a given solar radiation input and assuming a reflectance factor for the cleanliness of the solar collectors, thermal energy input can be determined from the efficiency of the collector loop as determined in the characterization experiments. In addition, during the pre-heat portion of a steam test

before boiling is initiated, the data generated provide a check of the collector performance characteristics.

2.3.5 Single Loop DSG Experiments

Prior to the beginning of an experiment, the tank was filled to the appropriate level with de-ionized water. Single loop direct steam generation involved setting the pump flow rate by establishing the VFD frequency and setting the pressure setpoint on the separator tank.

The pump was turned on and the collectors set to track the sun. Water recirculated from the separation tank through the solar loop and back to the tank. The fan coil unit was bypassed.

Temperatures in the solar loop increased until the saturation temperature of the water in the collectors reached saturation point when the water started to boil. The steam/water mixture was transported from the solar field to the separator tank. Steam was ejected to the atmosphere through the pressure control valve and the liquid water was recirculated back through the solar collectors.

Single-loop steam runs were carried out at various steam pressures and flow rates. For a given set of conditions, increasing the flow rate through the loop has no impact on the amount of steam generated, since that is simply a function of the solar thermal input. However, increasing flow did decrease steam quality since for the same amount of steam, the fraction of steam was lower at a larger total flow rate. Steam qualities during the experiments were from zero up to about 10 percent.

The goal of the single loop experiments in the first instance was to demonstrate that DSG at low pressures was actually feasible and that DSG can be carried out without material damage to the collector equipment and in a reasonably stable fashion. Second, the data gathered was to validate existing correlations or the basis for the derivation of new ones, if there was no agreement.

2.3.5.1 Simulated Multi-Low Steam Production

The multiple loop testing was to deliver experimental data to further understand the potential hydrodynamic interactions and the corresponding effects that can be expected from DSG loops connected in parallel. Understanding these hydrodynamic interactions between loops is essential as a means of designing the plant with specific hardware or control strategies that will passively and/or actively mitigate flow instabilities. Such instabilities can lead to a continuous increase in the production of saturated steam in some loops leading to potential dry out of the absorber tubes.

The bypass loop around the solar loop was installed to simulate the addition of loops in parallel to the single solar loop. A valve in this loop was used to impose mass flow rate and pressure perturbations to the DSG loop inlet conditions. The impacts were measured using the installed instrumentation as well as through direct observation.

CHAPTER 3

Results

3.1 Computational Fluid Dynamics (CFD)

3.1.1 Introduction

Computational fluid dynamics, usually abbreviated as CFD, is a branch of fluid mechanics that uses numerical methods and algorithms to solve and analyze problems that involve fluid flows (Wikipedia). The development of super-computers has allowed CFD to evolve into a powerful tool to understand the performance of fluid flows over aerofoils, the hulls of ships and wind turbine blades.

The fundamental basis of almost all CFD problems is the Navier–Stokes equations, which define any single-phase fluid flow. Because of the complexity of these equations, various techniques are employed to simplify the equations so that the run time on super computers is realistic in time scale and affordable in price.

For CFD solution techniques, the same basic procedure is followed.

- During preprocessing
 - The geometry (physical bounds) of the problem is defined.
 - The volume occupied by the fluid is divided into discrete cells (the mesh). The mesh may be uniform or non uniform.
 - The physical modeling is defined – for example, the equations of motion + enthalpy + radiation + species conservation
 - Boundary conditions are defined. This involves specifying the fluid behavior and properties at the boundaries of the problem. For transient problems, the initial conditions are also defined.
- The simulation is started and the equations are solved iteratively for steady-state or transient conditions.
- Finally a postprocessor is used for the analysis and visualization of the resulting solution.

DSG is a problem that never before has been investigated using CFD. DSG involves highly turbulent flow in two phases, the diameter of flow is relatively small so the wall effects are major, the flow is horizontal so gravitational forces are important and there is non-uniform heating of the perimeter wall. In addition, particularly at low steam pressures, the quality of steam changes significantly down the tube because of the flashing caused by pressure drop.

Given the complexity of the problem, various empirical approaches have been used to attempt to understand DSG pressure drop and fluid distribution through multiple flow loops especially as it influences tube dryout. Since tube dryout can cause structural failure of the absorber tube, a greater understanding of the conditions needed to avoid such failures is important. One aspect of this project was to employ CFD to enhance that understanding.

Dr. Olivier Desjardins of the University of Colorado, Boulder (CU) (now at Cornell University) gained his PhD from Stanford University, a noted center of CFD research. Professor Desjardin carried on his CFD research at CU and became an acknowledged expert in the field. With a clear understanding of the complexities involved, Dr. Desjardins, working with PhD graduate student Jeremy McCaslin, was confident that some progress could be made to enhance the understanding of DSG phenomena.

3.1.2 Colorado University Approach

After some investigation of the problem, the researchers at Colorado University (CU) decided to employ a modeling technique known as Large-Eddy Simulation (LES). This is a technique (Wikipedia) in which the smallest scales of the flow are removed through a filtering operation. This allows the largest and most important scales of the turbulence to be resolved, while greatly reducing the computational cost incurred by the smallest scales. This method requires greater computational resources than RANS (Reynolds-averaged Navier-Stokes methods), but is far cheaper than DNS (Direct Numerical Simulation). DNS resolves every scale of the solution, but is prohibitively expensive for nearly all systems with complex geometry or flow configurations.

The first step in CU's research effort on modeling two-phase flow was to verify the computational code starting with the least complex and more fundamental two-phase Pouseuille flow. Pouseuille flow considers laminar flow and does not take into account frictional effects of the wall. There is a non-slip condition between the inner pipe wall and the liquid flowing in the pipe.

The next step was to impose turbulent conditions on the flow to simulate and predict flow parameters at the proposed operating conditions of the DSG experimental solar loop. Velocity profiles in a 2D field of the liquid and gaseous phases (stratified flow) were correctly simulated by the code and validated against the analytical solutions to Pouseuille flow equations. Furthermore, when turbulent fluctuations were introduced into the flow, CU was able to define different flow regimes in the two-phase flow moving through the horizontal pipe. The expected stratified flow to stratified-wavy flow regime transitions were correctly calculated in the outputs from the simulations. By imposing higher fluid flow velocities, the code was able to move into regimes beyond the stratified-wavy flow pattern.

3.1.3 Colorado University Results

The results of the CU CFD research work is shown in the technical report attached in Appendix 2. To keep the work grounded in developments aimed at commercializing DSG technology, the focus is mainly on the predictions of the dry-out conditions. Two ranges of steam pressures were investigated. First, was the low pressure steam case peaking at about 10 bar that is the range of pressure used in much of industry. Second, was the high pressure case of 100 bar that is of interest for utility power generating applications.

The CU reports points out the limitations of such a short research effort, but nevertheless some important findings emerged. Most important was that a calculated Froude number dictates the thickness of the liquid film surrounding the top and sides of absorber tube. Furthermore, the thickness of this liquid film seems to be the predominant factor in determining the two-phase

flow regime and the potential for tube dry-out. A Froude number >1 is required to maintain annular flow and a liquid film on the complete circumference of the tube. The use of the Froude number is a complete new way of looking at two-phase flow regime transitions.

For the high pressure steam condition, the simulations indicated that mechanisms exist for sustaining a contiguous film around the wall. Three such mechanisms were identified:

1. droplet entrainment from the thicker layer of liquid at the bottom of the pipe and deposition near the top,
2. secondary gas flow in the circumferential direction generated by protrusions in the liquid surface and,
3. wave-pumping action that pushes liquid up the pipe walls.

At the lower pressure steam conditions, the simulations showed that a sustaining mechanism to keep the pipe wall wetted with liquid was absent. Any liquid pushed up the wall could not be maintained in place because the momentum of the steam passing through the tube was not sufficient to overcome the gravitational force on the liquid film draining it back to the bottom of the pipe.

A pictorial representation of the results of the CFD simulations is shown in Figures 3-1 and 3-2 for the high (85 bar) and low (11 bar) pressure steam conditions. Figure 3-1, shows that at high steam pressure, the vapor space is awash with the flow of liquid particles that maintains the liquid film on the wall against the force of gravity. In addition, at high steam pressure, vapor velocities in the two counter-current vortices are greater and serve to push fluid further up the wall even when the level of liquid at the bottom of the pipe is less.

Figure 3-2, shows a prediction of film thickness from the bottom of the pipe (0 on x-axis) to the top of the pipe (1 on x-axis). Corresponding with these values of film thickness is the probability of dryout conditions existing at points around the circumference of the pipe. It shows that the probability of dryout at low steam pressures is high, but much less likely at higher steam pressures even though the vapor fraction is much greater.

In a very short time, the CU researchers tackled a problem that had not been previously investigated using CFD and made a major contribution to the basic understanding of two-phase flow in horizontal pipes that could not be determined through any other means. The limitations of the study and the need for future work are readily acknowledged. For instance, it was assumed that as long as flow was turbulent that using Reynolds numbers much lower than actual values was acceptable; the length of the simulation was only about three pipe diameters; and, the impacts of thermal energy addition to the mixture or changes in steam quality were not considered. In addition, some of the results appear to contradict conventional correlations. For instance, the simulations show the potential for dry out at low steam pressures, whereas author plots of the progression of two-phase flow on the conventional flow regime map of Taitel and Dukler show a transition to annular flow. It is hoped that the funding of this initial work provides the impetus for future study.

Figure 3-1: Two-Phase Flow Velocity Profiles in Pipe at High (85 bar) and Low (11 bar) Pressures

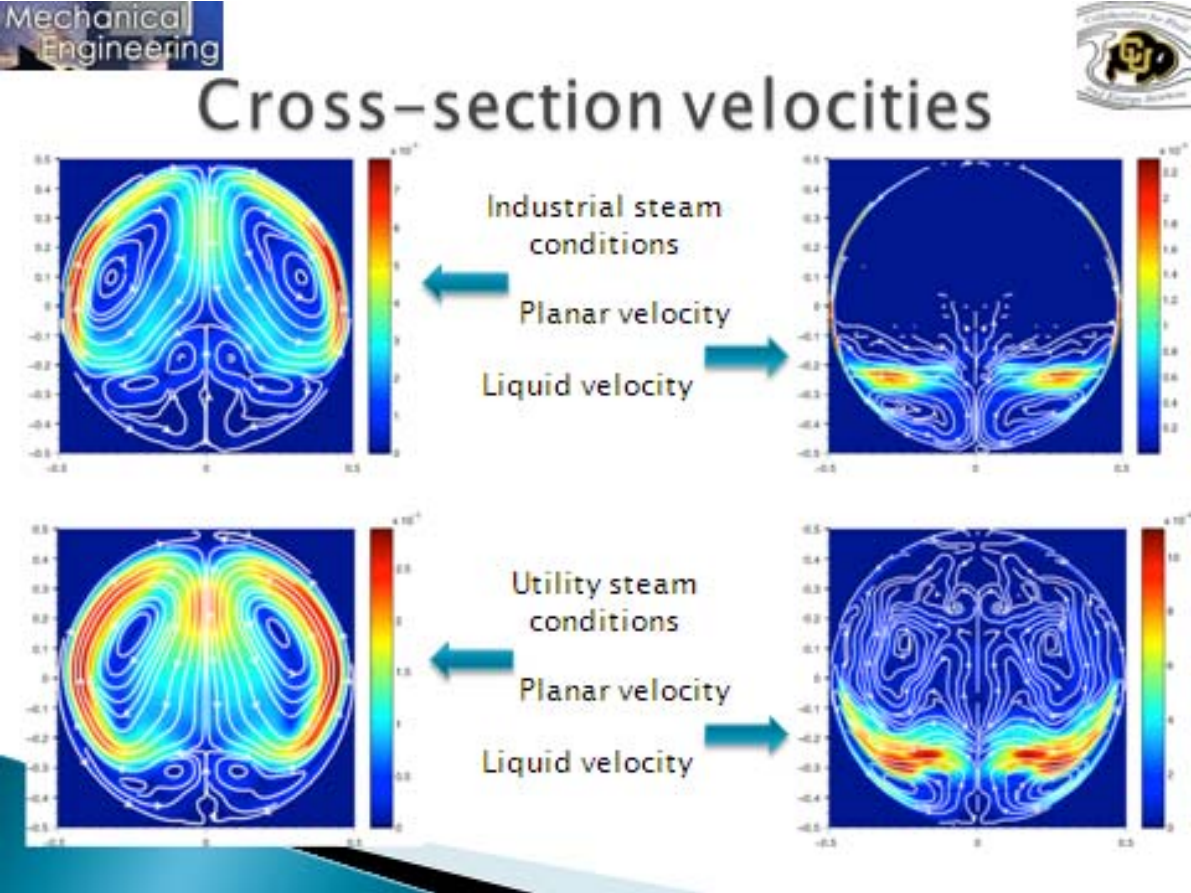
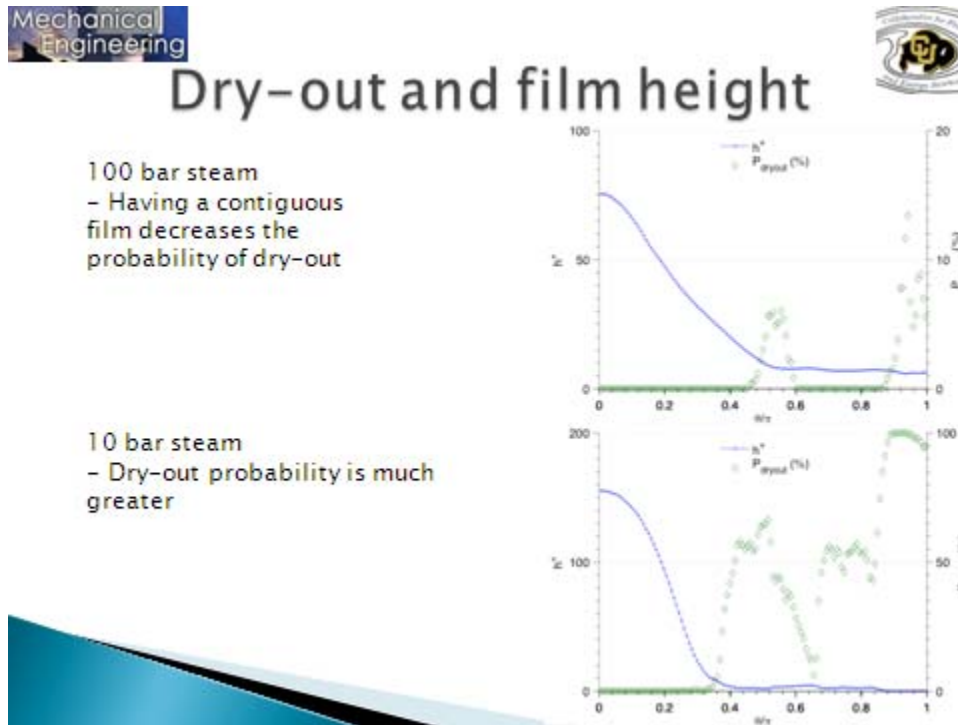


Figure 3-2: Two-Phase Flow in Pipe at High (85 bar) and Low (11 bar) Pressures Showing Film Thickness and Potential for Tube Dryout



3.2 Experimental DSG Program

3.2.1 Characterization of Test Loop with Liquid Flow

The test loop was first characterized for pressure drop. This testing was completed in the winter using a water/antifreeze mixture with the collectors in the face-down stow position. The conditions under which the tests were conducted are shown in Table 3-1. Pressure was measured using the 6 pressure transducers located around the loop in the locations shown in Figure 3-3. Between PT-003 and PT-005 for the inlet collector, and PT-006 and PT-008 for the outlet collector is a straight run of pipe each 50 m long. Between PT-005 and PT-006 are two flexible hoses and 18 ft of cross over pipe with fittings.

Flow was established by setting the variable frequency drive (VFD) on the circulating pump motor at a percentage of the line (60 Hz) frequency. At 60 Hz, the motor turned at 3600 rpm. Pump suction was from the tank open to the atmosphere so a few feet of head. Pump discharge pressure was measured with a pressure gauge.

Figure 3-3: Location of Pressure Transducers in DSG Flow Loop

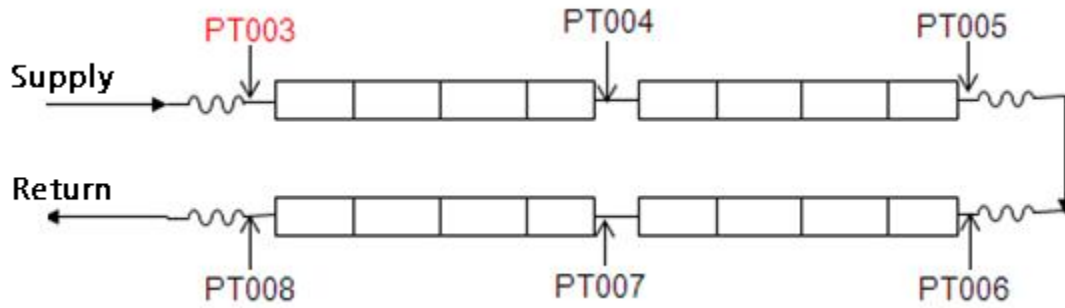


Table 3-1: Pump Discharge Pressure vs. Flow Rate

Motor frequency, %	Flow Rate, gpm	Pump Discharge, psig
10	10	6
20	14	10
30	18	14
40	22	20
50	26	24
60	29	32
70	33	40
80	36	48
90	40	56

Pressure measurements for different operating conditions are shown in Figure 3-4. The largest pressure drop within the loop was through the cross over piping.

Figure 3-4: Pressure in Flow Loop vs. Flow Rate

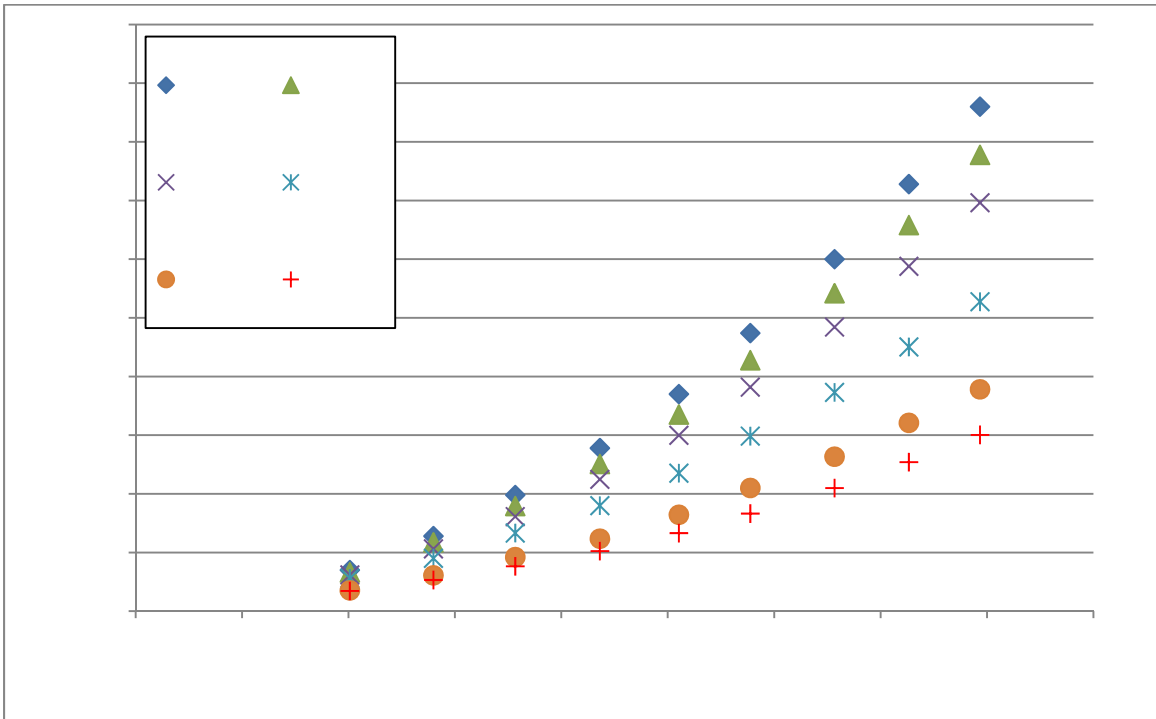
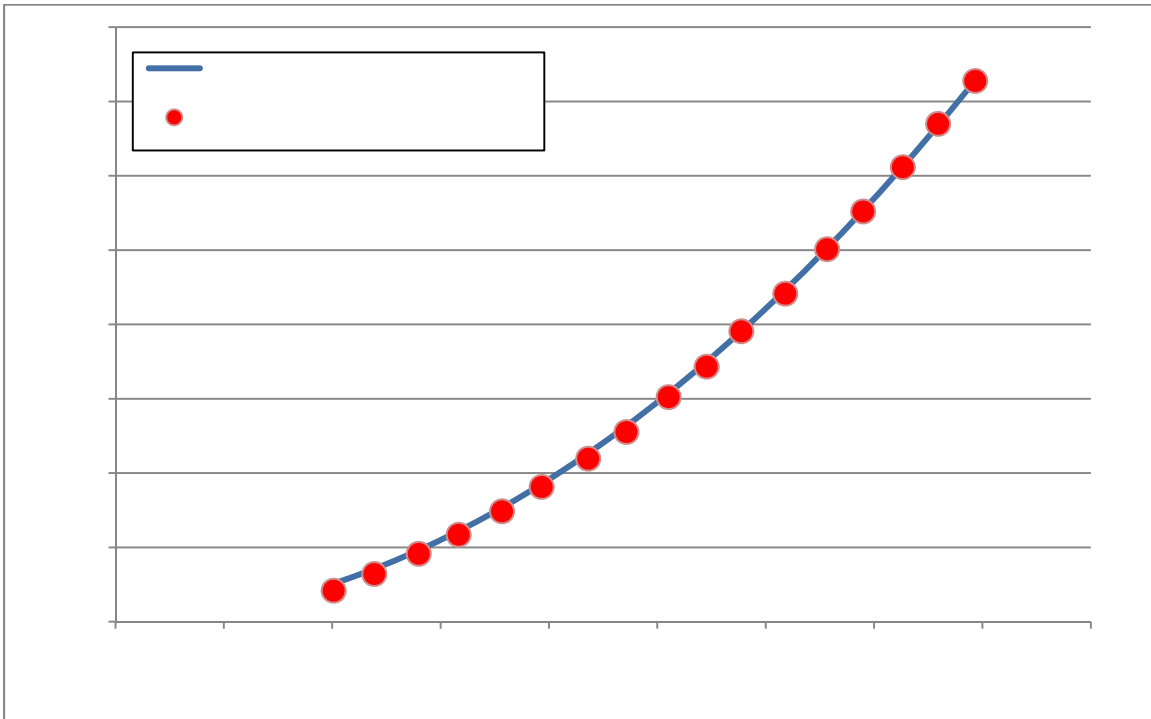


Figure 3-5, compares the measured pressure drop between PT003 and PT008 across the entire flow loop to the theoretical model, in which there is good agreement. This was expected because predictions of single-phase pressure drop are well validated. However, this result was an important first step in the theoretical analysis since the prediction of two-phase pressure drop is a modification of single-phase pressure drop.

Figure 3-5: Measured vs. Predicted Pressure in Flow Loop



Next the solar loop was characterized in terms of thermal performance and efficiency. First measurements were carried out in the winter using the anti-freeze mixture. However, in the spring, this heat transfer fluid was replaced with water that has better known thermodynamic properties. The measured data compared to theoretical models is presented below.

Figure 3-6, is an example of the initial test results using glycol. These test pointed out deficiencies in collector tracking that were corrected for later tests. Direct normal radiation measurements were made by Abengoa Solar's rotating shadow band pyranometer that is installed at the site. Efficiency was based on converting DNI to radiation in the collector aperture plane by multiplying by the cosine of the solar incident angle. No corrections were made for end losses and collector shading was zero at the time of the tests. The efficiency included the inlet and outlet piping between the solar loop and the instrumentation shed, and heat loss in the cross over piping.

Figure 3-6: All Day Performance of the Collector Test Loop—Measured DNI (W/m²) and Thermal Efficiency (%)

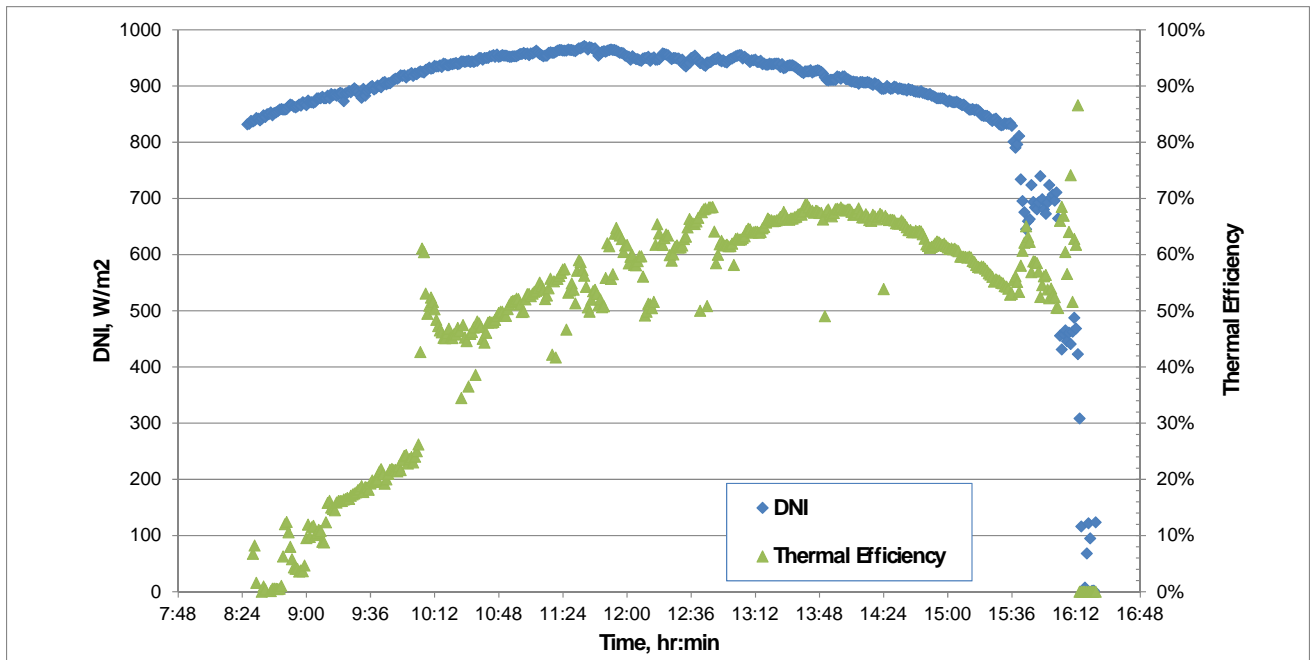
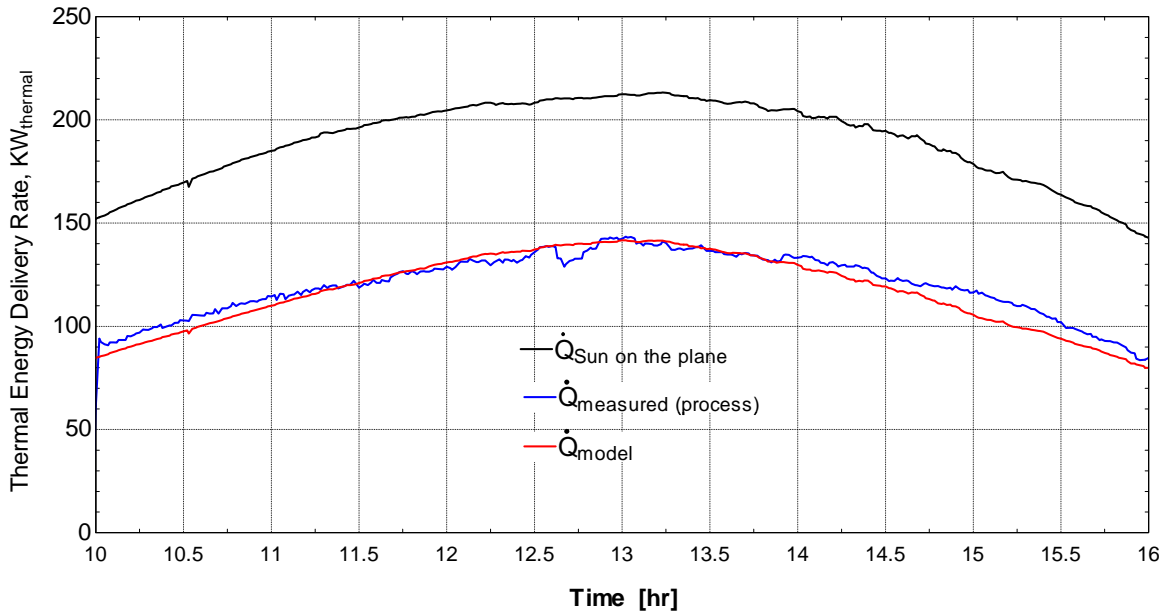


Figure 3-7, is an example of the results of the performance characterization using water in the collector loop. The measured results are compared against the theoretical predictions from the collector performance model.

Figure 3-7: Full Day Test Performance Test under Clear Sky Conditions—Solar Radiation, Measured and Predicted Thermal Energy Delivery



The correlation between the modeled thermal energy with the measured data is very good within +/- 1.5 hours from solar noon (between hours 11:30 and 14:00). Deviations in thermal output were due to imperfect collector tracking. Additional modifications to the tracking software were made to correct this. The model seems to be more conservative than the real system early in the morning and late in the afternoon. This deviation could probably be corrected by adjusting the incident angle modifier. However, the difference was not of concern for this study since the DSG experiments were conducted during the middle part of the day when conditions are most stable

Figure 3-8: Full Day Test Performance Test under Clear Sky Conditions—Solar Loop Inlet and Outlet Temperatures

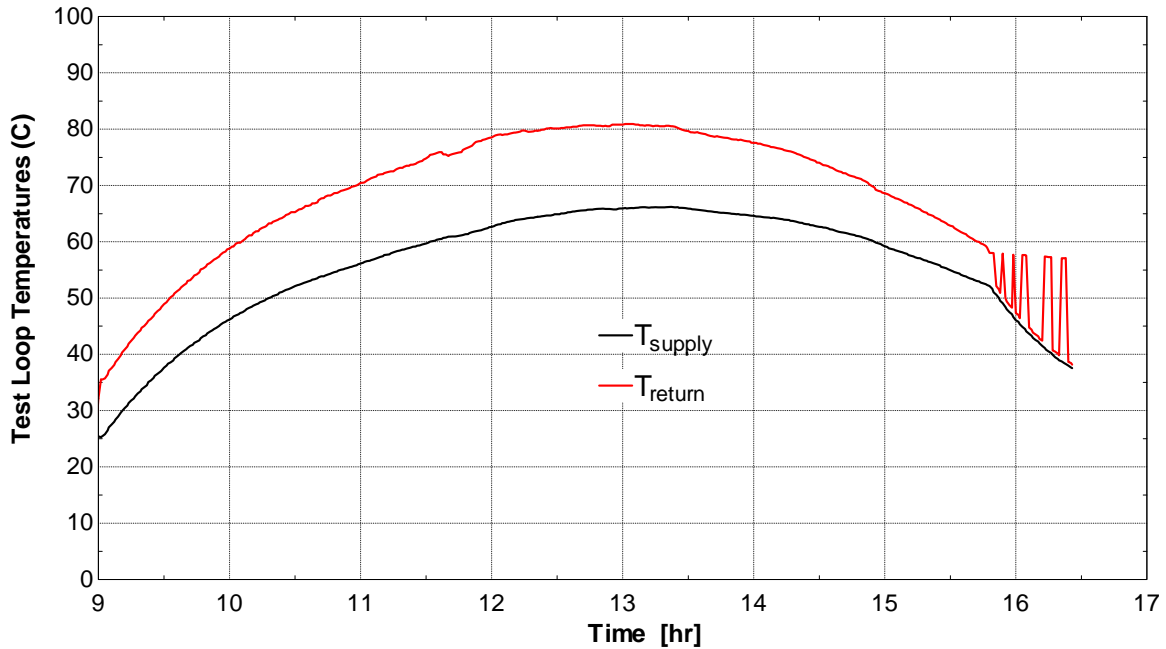


Figure 3-8, illustrates loop inlet and outlet temperatures during the test. The maximum temperature gain is approximately 15 degrees C corresponding to thermal energy delivery of about 140 kW.

The characterization tests validated the performance model. During steam generation in the absorber, the differential temperature across the loop is very small because most of the solar thermal energy input is converted into latent heat. The performance model fills this gap in the data by allowing the calculation of the energy content of the fluid at any point in the loop based on the inlet temperature and flow, direct normal radiation, incident angle, ambient temperature and the cleanliness of the concentrator reflector and receiver glass envelope.

3.2.2 Impacts of DSG on Equipment

As part of the experimental program, steam was generated at various steam pressures under a wide range of operating conditions. These tests allowed the impact of the boiling and two-phase fluid transport in the absorber tubes, and system piping and equipment to be evaluated.

Prior to this work, most research in DSG had been conducted at very high pressures to deliver steam for electrical generation. At low pressures, the density difference between water and water vapor is much greater than at higher pressures. Consequently, fluid velocities are much greater. In addition, at low pressures, a small difference in pressure creates a much larger difference in saturation temperature than at higher pressures. This causes liquid water to flash to steam during its transport down the receiver tube. Flashing is somewhat like water hammer that can be very violent.

Finally is the question of tube dryout. The theoretical analysis shows that the likelihood of dryout increases as pressure is reduced. Plotting of conditions at 10 bar steam generation on flow regime maps shows that some circumstances are close to the least desirable stratified flow regime. The CFD work suggests that at 10 bar, flow is indeed stratified since the Froude number is less than 1; the momentum of the vapor flow is insufficient to maintain a film of liquid around the tube circumference. Extending this analysis to low pressures would only increase the probability of tube dryout.

During the heating of a liquid in the absorber tube without phase change, there is no visible affect on the system piping. Only by detecting slight vibrations on exposed piping is it possible to tell that liquid is flowing through the tubes. However, the impact of steam generation is visible.

Closest to the loop outlet, where conditions are most severe, there is a slight vibration of the absorber tube. This vibration is absorbed by the flexible receiver supports that move slightly backwards and forwards by a small amount (less than 10 mm). The vibration works its way back, with less severity, along the absorber tube to the point where steam generation first begins. The wire rope connecting the two collectors in a drive string slightly vibrates also. Any movement to the collectors themselves is very slight and there is no indication of an impact on collector tracking. Since the tracking system employs a feedback mechanism from photosensors located on the receiver, vibrations that moved the collector even a small amount out of focus could cause the control system to react, mostly likely in an unstable fashion.

There is a flexhose at each end of an 8-module collector. These hoses absorb the movement between the rotating collectors and fixed piping system. They are made of convoluted, thin-wall bellows, and consequently are the weakest part of the piping system. They are of slightly smaller diameter than the absorber tube, and hence fluid velocities will increase during passage from the absorber tube. The hose at the loop outlet will suffer the most impact. It demonstrated similar vibrations to the absorber tube but at this point there have been no negative impacts, other than the significant effect on pressure drop. The long-term effect is unknown.

The heat transfer coefficient of flowing steam is much lower than flowing water. Hence, without cooling provided by a film of water, localized overheating of the dried out receiver could occur. Given our current state of knowledge, there is no means to understand exactly what is going on inside the absorber tube in terms of dryout. However, if localized overheating of the absorber tube were to occur, then this would show up as a discoloration of the selective surface, although it would take a temperature of around 300 C or more to affect this change. There is no evidence of a discoloration of the absorber tube in the test loop. A potential explanation follows. However, this explanation is for a tube in which there is flow, even if at a relatively low rate. Conditions of complete flow starvation in the loop, whereby the flow rate decreased to the point where it is almost entirely filled with vapor did not occur during our experiments. Theoretically, flow starvation is a potential result of multi-loop flow instabilities.

Generating steam at low pressures, even at low qualities, increases the possibility of tube dryout. However, low pressures mean that the collectors are operating at low temperatures.

For instance making 50 psig steam, the peak collector temperature will be some degrees C above about 150 C; making 150 psig steam some degrees above 185 C. Yet, to cause actual damage to the absorber tube, it would have to be heated to a temperature in excess of 600 F (316 C). In the pilot plant loop during experiments, it is possible that there were locations of stratified flow where the bottom of the tube had most of the liquid and the top of the tube was not always covered with a liquid film. However, inside the tube, conditions are turbulent, and boiling and flashing are liberating bubbles that serve to mix the liquid even more. (The CFD analysis considered tube wetting and liquid entrainment only in terms of momentum transfer without considerations of thermal energy input or flashing). Hence, it is postulated, should localized dryout occur, given all the turbulence in the fluid, that such a dryout condition is transient before the dry area is splashed with liquid. During that brief period of dry out, the degree of overheating would be minor and would be mitigated by conductive heat transfer in the metal absorber tube to cooler regions.

During start up of the solar system with a hot tank, the circulating pump experienced extremely high rates of temperature increase. However, no detrimental impacts were observed during the period when tests were being conducted. However, the Net Positive Suction Head (NPSH) requirements of the pump must be considered.

Overnight or during the down time between steam-generating tests, the steam separator tank cooled in temperature. After a single overnight, there was still usually positive pressure on the system. However, after longer periods, the condensation of steam produced a strong vacuum. This vacuum over water in the tank, close to the saturation point, could cause problems with the pump because of net positive suction head requirements (NPSH). In anticipation of this effect, the tank was elevated some feet above the pump suction. However, high vacuum affected the ability of the circulating pump to draw suction. Thus, in a commercial design, it would be necessary to minimize vacuum conditions in the separator tank. One solution would be to back-feed steam from the process delivery header into the tank system.

The graphs of DSG data that are shown later in this report illustrate the pulsating nature of the pressure measurements that reflect the boiling taking place in the absorber tube. These pulsations took their toll on the pressure transducers that were installed along the absorber tube. During the course of the experiments, numerous of them failed in a mode that short-circuited their electronics. The fact that these instruments were close to the focal point of the parabola and subjected to concentrated solar radiation added to the stress. Pressure transducers would not be installed in the absorber of a commercial system. However, they are deployed around the balance of plant equipment. For these few instruments, more robust and expensive transducers could be deployed with the goal of improving reliability. Measurement of temperature at the center of the absorber tubes is normal, but no failures of the temperature elements occurred during the experimental program.

Overall, based on the observations at the pilot plant, the mechanical impacts observed during DSG are minor and would not hinder the application of the technology.

3.2.3 DSG Operations

The pilot plant was operated in a totally automatic mode for the DSG experiments and the generation of steam became routine. The only intervention was to set the desired steam pressure and initial flow rate prior to the start of an experiment. Operations followed a similar pattern regardless of the initial conditions of low and steam pressure. These operations are described here and can be followed in the performance graphs that follow.

At the beginning of the day, if there is sufficient sun and there are no safety parameters out of range, the control system starts the circulating pump, verifies flow and initiates tracking of the collectors. Energy is absorbed into the liquid water circulating through the solar loop. Energy input to the system is determined by the angular orientation of the collectors to the sun, sun intensity and the efficiency of the collector system. Under single-phase conditions, the outlet of the loop is at the highest temperature and lowest pressure. Energy is transported to the separator tank causing the entire system to increase in temperature. Because of thermal expansion of the liquid water and the increase in vapor pressure of the hot water, pressure increases also. With solar energy input to the system and no energy extraction, a point is reached when water entering the tank is at its saturation pressure and temperature. At that point, water entering the tank flashes to a mixture of steam and water. The production of steam causes a much greater rate of pressure increase than single-phase, liquid expansion so once boiling is initiated pressures increase rapidly. Once pressure in the tank attains the set point of the pressure-regulating valve, the valve opens to maintain the pressure in the tank and steam is ejected to atmosphere. The large volume of the tank and the tangential entry of the water/steam mixture into the tank ensure efficient steam separation and the delivery of dry saturated steam to what in normal circumstances would be the industrial process.

Once steam is produced, solar energy input no longer causes an increase in system temperatures; all the energy is converted into the latent heat of steam. The pressure/temperature saturation point of the fluid flowing through the collector loops (and hence the point where the phase change process begins) moves upstream from the tank and into the absorber tubes of the collectors.

3.3 Results of Single-Loop DSG Experiments

Steam was generated at various steam pressures under a wide range of operating conditions and is illustrated in the following graphs. They all follow a similar trend and these trends are outlined below, together with specifics related to the actual experiments.

Figures in Appendix D, D-1, D-2 and D-3 illustrate steam generation over a complete day of operation at a pressure of 5.9 bar. The data are presented as one minute averages of data taken about every controller scan of about 3 seconds. All the pressures in the flow loop are shown, but unfortunately, the two temperatures at the center of the absorber tubes were not being recorded when these data were taken.

Figure D-1 illustrates the rapid ramp up in system temperatures after the tank was refilled with cold water. It took almost two hours to heat up this large volume of water before steam

generation began. However, heat up took place during the least favorable solar conditions at the beginning of the day.

During heat up, there is a temperature gradient through the loop increasing in temperature from the tank to the field outlet. The flow of water was relatively constant. After steam generation begins, conditions change dramatically. The loop inlet, the tank and the steam temperatures are essentially the same. (Any difference is because the tank is not perfectly mixed.) In the first row of the loop, temperature increases from the inlet to the cross over pipe. From there, temperatures decrease as pressure decreases and liquid water flashes to steam. The loop outlet temperature is very constant as it is tied closely to the steam saturation temperature in the tank. The difference in temperature between the loop outlet and the tank is due to the effect of steam flashing in the return pipe as its pressure decreases.

The generation of steam and the increasing pressure drop causes a large decline in the loop flow rate. Flow rate is inversely proportional to sunlight intensity and the amount of thermal energy generated.

Figure D-2 illustrates pressures through the solar loop. Until steam generation commences, pressure drop through the loop is low because it is determined by liquid phase flow only. With steam generation, pressure drop in the liquid region of the first collector remains low. However, pressure drop through the two flexhoses, fittings and pipe of the crossover line is significant. Pressure drop through the straight absorber tube of the second collector is large also; pressure drop through the second half being greater than through the first half of the absorber. There is also a large pressure drop through the piping from the end of the second collector to the steam separator tank.

The centrifugal circulating pump was run at a fixed speed under the control of a variable frequency drive. The onset of steam generation and the large increase in pressure drop about halves the flow rate. This increases the head on the pump and its discharge pressure. As solar energy input and steam generation decline towards the end of the day, flow rate increases correspondingly. However, pressures and temperatures in the steam generating region are relatively constant because both are tied to saturated steam conditions in the separator tank.

Figure D-3 shows the strong correlation between sun intensity (the startup sensor voltage \times cosine of incident angle) and system flow rate and pressure drop.

Figures D-4, D-5 and D-6 illustrate steam generation at a higher pressure of 8 bar. The pattern of the data is the same as in the previous three graphs. All the data confirm the conclusions derived from the theoretical analysis listed in Section 2.3.2. In terms of thermal performance, temperatures are only slightly above the steam saturation temperature. For the 5.9 bar steam, the peak temperature in the loop was 11.5 C above the steam temperature; for the 8 bar steam case, the difference was 7.5 C.

In both cases, the initial single phase flows and peak sun intensities were similar. During steam generation, the differential pressure through the loop was also about the same for the two cases. Flow rates caused by the increased pressure drop due to steam generation declined by about

half, with a slightly greater decline at the higher steam pressure. Since the pressure drop caused by steam generation also declined by about half, the power consumed by the pump before and after steam generation would be similar. This fact suggests an operational strategy to minimize pump electricity use.

In single phase operations, flow rates through the solar field are maintained high to keep system operating temperatures as low as possible. Maintaining the same high flow rate in two-phase flow would increase the required pump head considerably, and would increase system operating pressures and temperatures. The resultant higher temperatures and pump power are the opposite of the desired outcome. Thus, setting aside all considerations of tube dryout and potential inter-loop instabilities, a strategy might be to establish pump flow at a rate such that the initial point of steam generation is some way into the collector loop. Based on the data, this flow rate might be in the range of 10 – 15 gpm (2.3 to 3.4 m³/h) one-third to one-half of the maximum design flow rate for a liquid. The VFD on the pump would attempt to maintain this flow against the back pressure produced by two-phase flow.

The previous data shown were examples of experimental runs. They demonstrated that the system responded to changes in solar radiation in a predictable and stable fashion. Figures D-7, D8 and D9 illustrate the impact of a sudden change in the steam pressure from 9 to 10 bar.

The system came up to temperature to generate steam at 9 bar. Flow rate declined in the usual manner. Flow rate continued to decrease gradually as the level of solar radiation incident on the collector increased towards solar noon and normal incidence (see Figure D-9). The imposed step change in the pressure control of the steam separator tank temporarily stopped steam generation and increased flow through the loop. Thermal energy input to the system continued, however, so increasing in pressure in the tank to 10 bar. Flow rate declined again as steam generation was re-established.

The experiment was repeated going from steam at 4.3 to 5.9 bar. Throughout all these changes, the system responded in a stable and predictable fashion.

3.4 Results of Simulated Multi-Loop DSG Experiments

The potential instabilities arising from the design of large-scale solar systems arranged as many repeating loops in parallel was discussed previously. The pilot plant was built with a bypass loop from the pump discharge back to the tank, in parallel to the loop through the solar field. The bypass loop was designed to simulate the presence of the other flow loops in a larger solar field.

To conduct an experiment in the bypass mode of operation, the frequency of the pump was set and the flows through the two loops adjusted to the desired rates. The results of such an experiment are shown in Figures D-10, D-11 and D-12.

The most noticeable result is the impact of steam generation on the two flows, seen most clearly in Figure D-12. Prior to steam generation, temperatures and pressures are increasing. Flow through the loop is increasing slightly and there is a slight decrease in flow through the bypass.

As steam generation begins, there is a large increase in the pressure drop through the collector loop. This causes an overall reduction in flow output by the pump. Flow from the pump divides to equalize the pressure drop through the two loops. Thus, flow through the bypass increases and flow through the collector loop decreases.

The pressure distribution in the solar loop with bypass follows the same pattern as single loop flow, except for the interaction between the two loops caused by variations in sun intensity. There was considerable variation in the sun intensity during the experiment. Pressure distribution and flow rates responded predictably, but throughout all the changes the system was stable.

Figures D-13, D-14 and D-15 illustrate the generation of steam in bypass mode at the lower end of the pressure range mostly commonly used in industry (50 and 87 psig). Theoretically using DSG to produce steam at such low pressures should be more challenging than generation at higher steam pressures.

Figure D-13 shows a temperature increase from the loop inlet to the center of collector 1. There is little additional increase at the center of the loop indicating that the onset on boiling was somewhere in the second half of collector 1. There is a significant decrease in temperature from the center of the loop to the center of collector 2 and a greater decline from the center of collector 2 to the outlet of collector 2. The maximum differential temperature in the solar loop from the inlet to the center cross over is about 12.4 C. This compares with a maximum differential during the single phase heat up between the outlet and inlet of the loop of about 18.4 C.

The average temperature of the solar loop during steam generation was about 152.5C. This is only 5.7 C above the steam delivery temperature of 146.8 C. In the conventional steam generating process using an unfired steam generator, the inlet temperature would be about 8 C higher than the steam temperature. Based on the differential noted above, the average solar field temperature would be about 17.2 C above the steam temperature. Thus, a DSG system should be more efficient than a conventional solar steam-generating system because of lower temperature operations.

Figure D-14 shows the distribution of pressure around the loop. The pressure transducer at the inlet to row 1 had failed, but since single phase flow exists to the center of row 1, the pressure at the center of row 1 should be very similar to the inlet. The peak pressure in the loop was around 520 kPa, compared to the steam pressure of 345 kPa; a difference of 175 kPa. Based on the conditions in a conventional solar steam plant, the peak collector temperature would be around 173.2 C. The saturation pressure of such water is about 855 kPa; 510 kPa above the steam generating pressure.

The operating pressure of the conventional system needs to be considerably more because additional pressure must be added to ensure that boiling does not occur anywhere in the system. 100 kPa seems a reasonable margin of safety. In addition, the pressure to suppress boiling must be maintained all the way back to the outlet of the solar field, so the pressure drop in these return lines must be added to the pressure needed to suppress boiling. Thus the

operating pressure of a conventional system generating 345 kPa steam is in the range of 1000 kPa at the solar field outlet and even greater at the solar field inlet and the pump discharge. Greater analysis needs to be conducted for a commercial system design, but the data presented confirms that a DSG system operates at a lower pressure and temperature than a conventional solar steam plant. Such advantages should translate into better performance and lower capital cost.

Figure D-15 shows details of flow rate, loop pressure drop--from the center of collector 1 to the absorber at the exit of the loop, and sun intensity. It also clearly illustrates the impact of sun intensity on steam generation and the impact of increased steam generation on flow through the solar loop and bypass.

CHAPTER 4

Future Work

The experimental program has produced much unique operational data measuring conditions of two-phase flow in horizontal pipes. Future work is required to analyze these data. The first goal of the data analysis would be to test theoretical models to see whether they can be extended into the lower pressure steam regimes presented in this study. If these theoretical models do not produce the required level of accuracy, then the goal would be to derive the necessary modifications to achieve satisfactory correlation.

The models of two-phase flow pressure drop would be used to design the pipe network of a commercial DSG plant. The behavior of this network would be simulated under conditions aimed at reproducing possible real life scenarios. Conditions likely to cause dry out would be investigated by transposing conditions derived from the simulations onto flow regime maps. Conditions likely to create flow instabilities would be investigated by plotting curves of pressure drop versus mass flow looking for inflection points where increasing flow reduces pressure drop.

The network model would also be used as a means of testing techniques to prevent flow instabilities. The goal would be to use passive techniques in contrast to the use in CSP plants of flow meters and control valves on each loop. These valves are used to force a given flow through each loop, but are probably not affordable for an industrial solar steam system. Passive techniques that have been described in the literature include the use of orifices at the entrance to each loop.

It is also hoped that the initial work using CFD to investigate this complex problem will provide the stimulus for future work.

The proposed commercial plant design would be used as the basis for economic and performance comparisons with conventional solar steam plants. The designs should illustrate the promise of DSG technology, to significantly reduce the cost of solar steam by reducing system installed capital costs and increasing thermal performance.

The final step of future work is gain acceptance of DSG technology. This would probably require the construction of a first commercial demonstration plant. A technology with an enhanced competitive position with respect to natural gas will greatly assist marketing efforts into the California food processing industry. Increasingly in the future, the use of renewable technologies will be driven by the need to reduce carbon footprints.

CHATER 5: Conclusions

The conclusions of this report are:

- Researchers at the University of Colorado, Boulder applied Computational Fluid Dynamic techniques to DSG. They determined that a calculated Froude number was the predictor of the thickness of the liquid film and the potential for dryout.
- A DSG system will operate at a lower pressure and lower temperature than a conventional solar steam-generating system.
- DSG has the potential to reduce system capital costs while at the same time delivering increased thermal output.
- The direct generation of steam is relatively stable under a range of operating conditions and imposed perturbations brought about by changes in solar radiation and flow rate.
- There is no evidence of mechanical damage caused by DSG to solar system components.
- Future work is required to correlate the data and to derive commercial system designs.
- Commercialization requires that a demonstration in a commercial plant be built to prove the viability of the technology to industry.

GLOSSARY

BTU	British Thermal Unit
CFD	Computational Fluid Dynamics
PV	Photovoltaics
PIER	Public Interest Energy Research
RD&D	Research, Development, and Demonstration

APPENDIX A: References

- Eck, M., Steinmann, W. "Modeling and design of direct solar steam generating collector fields". Journal of Solar Energy Engineering. August 2005, Vol. 127, 371-380.
- Spedding, P. L., Benard, E., Donnelly, G. F.. "Prediction of pressure drop in multiphase horizontal pipe flow". International communications in heat and mass transfer. 33 (2006) 1054-1062.
- Garcia, P., Sanchez, M., Blanco, M., Valenzuela, L. "Validation of a dynamic model for direct steam generation in parabolic troughs using data from the DISS installation". SolarPaces Conference 2010.
- Natan, S., Barnea, D., Taitel, Y.. "Direct steam generation in parallel pipes". International Journal of Multiphase Flow 29 (2003) 1669-1683.
- Pye, J., Morrison, G., Behnia, M.. "Pressure drops for direct steam generation in line-focus solar thermal systems". Clean Energy – ANZSES 2006.
- Zarza, E., "The DISS Project: Direct Steam Generation in Parabolic Troughs Operation and Maintenance Experience – Phase I & II." Proceedings of Solar Forum 2001.
- Whalley, P. B.. "Boiling, condensation, and gas-liquid flow". Department of Engineering Science, University of Oxford. Clarendon Press – Oxford. 1987.
- Odeh, S. D., Behnia, M., Morrison, G. L.. "Hydrodynamic Analysis of Direct Steam Generation Solar Collectors". School of Mechanical and Manufacturing Engineering. The University of New South Wales. ASME 2000.
- Martinez, I., Almanza, R.. "Experimental and Theoretical Analysis of Annular Two-Phase Flow Regimen In Direct Steam Generation for a Low Power System". Universidad Autonoma de Mexico. Solar Energy 2006.
- S. I. Kosterin, "An investigation of the influence of the diameter and inclination of a tube on the hydraulic resistance and flow structure of gas-liquid mixtures," Izvest. Akad. Nauk. SSSR, Otdel Tekh Nauk, vol. 12, 1949.
- G. E. Alves, "Cocurrent liquid-gas flow in a pipe-line contactor," Chem. Eng. Prog, vol. 50, no. 9, p. 449456, 1954.
- O. Baker, "Designing for simultaneous flow of oil and gas," Oil and Gas Journal, vol. 53, p. 185195, 1954.
- L. I. Korsakov, "Some characteristics of the flow of a two-phase mixture in a horizontal pipe," Zhur. Tekh. Fiz, vol. 12, p. 65469, 1952.
- C. J. Hoogendoorn, "Gas-liquid flow in horizontal pipes," Chemical Engineering Science, vol. 9, pp. 205-217, Feb. 1959.

- V. Kadambi, "Stability of annular flow in horizontal tubes," *International Journal of Multi-phase Flow*, vol. 8, no. 4, p. 311328, 1982.
- G. Tryggvason, B. Bunner, A. Esmaeeli, D. Juric, N. Al-Rawahi, W. Tauber, J. Han, S. Nas, and Y. J. Jan, "A Front-Tracking method for the computations of multiphase flow," *Journal of Computational Physics*, vol. 169, pp. 708{759, May 2001.
- O. Desjardins, "Numerical methods for liquid atomization and application in detailed simulations of a diesel jet," 2008.
- R. T. L. Jr., "On the direct numerical simulation of two-phase flows," *Nuclear Engineering and Design*, vol. 239, pp. 867{879, May 2009.
- R. I. Issa and M. H. W. Kempf, "Simulation of slug flow in horizontal and nearly horizontal Pipes with the two-fluid model," *International journal of multiphase flow*, vol. 29, no. 1, p. 6995, 2003.
- M. Bonze and R. I. Issa, "On the simulation of three-phase slug flow in nearly horizontal pipes using the multi-fluid model," *International Journal of Multiphase Flow*, vol. 29, no. 11, p. 17191747, 2003.
- M. Bonizzi and R. I. Issa, "A model for simulating gas bubble entrainment in two-phase horizontal slug flow," *International Journal of Multiphase Flow*, vol. 29, no. 11, p. 16851717, 2003.
- J. M. Rodriguez, "Numerical simulation of two-phase annular flow," 2009.
- J. M. Mandhane, G. A. Gregory, and K. Aziz, "A flow pattern map for gas{liquid flow in horizontal pipes," *International Journal of Multiphase Flow*, vol. 1, pp. 537-553, Oct. 1974.
- Y. Taitel and A. E. Dukler, "A model for predicting flow regime transitions in horizontal and near horizontal gas-liquid flow," *AIChE Journal*, vol. 22, no. 1, pp. 47-55, 1976.
- GAS-LIQUID FLOW." [http://www.thermopedia.com/toc/chapt g/GAS-LIQUID FLOW.html](http://www.thermopedia.com/toc/chapt%20g/GAS-LIQUID%20FLOW.html).
- V. P. Carey, *Liquid-vapor phase-change phenomena: an introduction to the thermophysics of vaporization and condensation processes in heat transfer equipment*. Taylor and Francis, 2008.
- R. W. Lockhart and R. C. Martinelli, "Proposed correlation of data for isothermal two-phase, two-component flow in pipes," *Chem. Eng. Prog*, vol. 45, no. 1, p. 3948, 1949.
- C. D. G. King, *Heat Transfer and Pressure Drop for an Air-Water Mixture Flowing in a 0.737 inch ID Horizontal Tube*. PhD thesis, MS Thesis, University of California, Berkeley, CA, 1952.
- M. Ishii, *Thermo-fluid dynamic theory of two-phase flow*. Eyrolles, 1975.

- J. J. Ginoux, Two-phase flows and heat transfer with application to nuclear reactor design problems. Hemisphere Pub. Corp., 1978.
- W. H. McAdams, W. K. Woods, and R. L. Bryan, "Vaporization inside horizontal tubes-II-benzene-oil mixtures," *Trans. ASME*, vol. 64, no. 3, p. 193200, 1942.
- D. Chisholm and A. D. K. Laird, "Two-phase flow in rough tubes," *Trans. ASME*, vol. 80, no. 2, p. 276286, 1958.
- D. Butterworth, "A comparison of some void-fraction relationships for co-current gas-liquid flow," *International Journal of Multiphase Flow*, vol. 1, no. 6, p. 845850, 1975.
- R. C. Martinelli and D. B. Nelson, "Prediction of pressure drop during forced circulation boiling of water," *Recent advances in heat and mass transfer*, p. 318, 1961.
- C. J. Baroczy, "SYSTEMATIC CORRELATION FOR TWO-PHASE PRESSURE DROP.," in *Chem. Eng. Progr., Symp. Ser.*, 62: No. 64, 232-49 (1966)., 1966.
- M. Eck and W. D. Steinmann, "Modeling and design of direct solar steam generating collector fields," *Journal of Solar Energy Engineering*, vol. 127, p. 371, 2005.
- L. Friedel, "Improved friction pressure drop correlations for horizontal and vertical two-phase pipe flow," in *European two-phase flow group meeting*, Paper E, vol. 2, 1979.
- S. Natan, D. Barnea, and Y. Taitel, "Direct steam generation in parallel pipes," *International Journal of Multiphase Flow*, vol. 29, pp. 1669-1683, Nov. 2003.
- J. Pye, G. Morrison, and M. Behnia, "Pressure drops for direct steam generation in line-focus solar thermal systems,"
- P. Spedding, E. Benard, and G. Donnelly, "Prediction of pressure drop in multiphase horizontal pipe flow," *International Communications in Heat and Mass Transfer*, vol. 33, pp. 1053-1062, Nov. 2006.
- J. R. Pletcher and H. M. Jr., "Heat transfer and pressure drop in horizontal annular two-phase, two-component flow," *International Journal of Heat and Mass Transfer*, vol. 11, pp. 1087-1104, July 1968.
- J. Wurtz et al., "An experimental and theoretical investigation of annular steam-water flow in tubes and annuli at 30 to 90 bar," *RISO report*, vol. 372, 1978.
- G. K. Batchelor, *Collected Works of G.I. Taylor*. Cambridge University Press, 1958.
- G. I. Taylor, "Generation of ripples by wind blowing over a viscous fluid," *The Scientific Papers of G.I. Taylor*, p. 24454, 1962.
- D. Kim, A. J. Ghajar, R. L. Dougherty, and V. K. Ryali, "Comparison of 20 two-phase heat transfer correlations with seven sets of experimental data, including flow pattern and tube inclination effects," *Heat Transfer Engineering*, vol. 20, no. 1, p. 1540, 1999.

- D. Kim, A. J. Ghajar, and R. L. Dougherty, "Robust heat transfer correlation for turbulent gas-liquid flow in vertical pipes," *Journal of Thermophysics and Heat Transfer*, vol. 14, no. 4, p. 574578, 2000.
- D. Kim and A. J. Ghajar, "Heat transfer measurements and correlations for air-water flow of different flow patterns in a horizontal pipe," *Experimental Thermal and Fluid Science*, vol. 25, no. 8, p. 659676, 2002.
- J. Kim and A. J. Ghajar, "A general heat transfer correlation for non-boiling gas-liquid flow With different flow patterns in horizontal pipes," *International Journal of Multiphase Flow*, vol. 32, no. 4, p. 447465, 2006.
- A. J. Ghajar and C. C. Tang, "Heat transfer measurements, flow pattern maps, and flow visualization for Non-Boiling Two-Phase flow in horizontal and slightly inclined pipe," *Heat Transfer Engineering*, vol. 28, no. 6, p. 525540, 2007.
- C. E. Dengler and J. N. Addoms, "Heat transfer mechanism for vaporization of water in a vertical tube," in *Chemical Engineering Progress Symposium Series*, vol. 52, p. 95103, 1956.
- S. A. Guerrieri and R. D. Talty, "A study of heat transfer to organic liquids in Single-Tube, natural circulation, vertical tube boilers," in *Chemical Engineering Progress Symposium Series*, vol. 52, p. 6977, 1956.
- L. sun Tong and Y. S. Tang, *Boiling heat transfer and two-phase flow*. Taylor & Francis, 1997.
- P. Spedding and D. Spence, "Flow regimes in two-phase gas-liquid flow," *International Journal of Multiphase Flow*, vol. 19, pp. 245-280, Apr. 1993.
- Rodriguez, M. J.. "Numerical Simulation of Two-Phase Annular Flow". 2009. A thesis submitted to the graduate faculty of Rensselaer Polytechnic Institute in partial fulfillment of the requirements for the degree of Doctor of Philosophy.
- L.M. Murphy and E. Kenneth May. "Steam Generation in Line-Focus Collectors: A Comparative Assessment of Thermal Performance, Operating Stability and Cost Issues". Solar Energy Research Institute, Golden, CO, SERI/TR-632-1311, April 1982.
- R. J. Pederson and E. Kenneth May. "Flow Instability During Direct Steam Generation in a Line-Focus Solar Collector System". Solar Energy Research Institute, Golden, CO, SERI/TR-632-1354, March 1982.

APPENDIX B: First-Principle-Based Modeling of Direct Steam Generation Final Report

Olivier Desjardins. "First-principle-based modeling of Direct Steam Generation, Final Report",
September 2, 2011, Sibley School of Mechanical and Aerospace Engineering, Cornell
University, Ithaca, NY 14853

APPENDIX C:
Design of DSG Solar Pilot Plant

APPENDIX D: Results of DSG Experiments